



Environment  
Canada

Environnement  
Canada

Fisheries  
and Marine  
Service

Service des pêches  
et des sciences  
de la mer

# FERRO - CEMENT for CANADIAN FISHING VESSELS

Volume 4

DFO - Library / MPO - Bibliothèque



09039267

#64

Canada. Fisheries and  
Marine Service.  
Industrial Development Branch  
TECHNICAL REPORT



Vessels and Engineering Division  
Industrial Development Branch

10111

This publication is number 64  
in the Technical Report Series  
of the Industrial Development Branch

# FERRO - CEMENT for CANADIAN FISHING VESSELS

Ottawa / Hull 1973

Volume 4

*prepared by*  
The British Columbia Research Council  
Vancouver, Canada

*for*  
Vessels and Engineering Division  
Industrial Development Branch  
Fisheries and Marine Service  
Environment Canada

*Project Officer*  
G. M. Sylvester

*Division Chief*  
H. A. Shenker



*Opinions expressed and conclusions reached  
by the author are not necessarily endorsed  
by the sponsors of this project*

Issued under the  
authority of the  
Honourable Jack Davis, P.C., M.P.,  
Minister,  
Environment Canada

Commercial Letter & Litho Inc. - 03KT.KA-305-3-3253

TABLE OF CONTENTS

	<u>Page</u>
A. INTRODUCTION	1
B. SUMMARY	1
C. TEST PROGRAM	3
1. Preparation of Test Panels	3
2. Tensile Testing	6
3. Flexure Testing	8
(a) Procedure and Test Results	8
(b) Interpretation and Discussion	10
4. Tests to Establish Stress/Strain Hysteresis Effect	11
5. Tests to Examine Critical Crack Width	12
6. Seawater Exposure Tests on Painted Specimens	13
(a) Marine Tidal Exposure	13
(b) Laboratory and Seawater Exposure	15
D. GAPS IN THE TECHNOLOGY OF FERROCEMENT	15
E. REVIEW OF LITERATURE	16
REFERENCES	19
TABLES	20
FIGURES	44

## A. INTRODUCTION.

Several years ago the Fisheries Service, Canada Department of the Environment, perceived the considerable interest of amateur boat-builders in the construction of boats using a rod and wire mesh skeleton plastered with a cement/sand mortar, i.e., ferrocement. Some of these vessels were being used in the fishing industry, and the Fisheries Service sponsored a series of studies<sup>(1,2,3,4)</sup> on Ferrocement for Canadian Fishing Vessels to develop a "feel" for the general engineering properties of this composite material in its many structural variations.

Previous studies under the sponsorship of the Fisheries Service considered the influence, in a very general way, of several kinds of wire mesh, rods, cement, sand, and admixtures on flexural and impact strength and on resistance to freeze-thaw and marine exposures. Resistance of various paint coatings or ferrocement to the marine environment and the behaviour of ferrocement under flexural fatigue loads and under stresses imposed by bolted fastenings were examined. A mathematical model for a composite material of cement/sand mortar and steel mesh and rod reinforcements was posed and a bibliographic file of ferrocement literature was initiated and maintained.

This report covers new work on Ferrocement for Canadian Fishing Vessels carried out in the 1972-73 program under the sponsorship of the Fisheries Service.

## B. SUMMARY.

The present work follows the general approach used in previous studies but with emphasis on: (1) obtaining some data especially in flexure which can be used at a later date in a mathematical model, (2) obtaining some information on the relationship between crack width and corrosion attack of the mesh in seawater, (3) continuing the marine exposure tests on paint-coated specimens, (4) maintaining the bibliographic file, and (5) providing a technical information service to persons interested in ferrocement for boat-building and other purposes.

The proposed program proved unduly ambitious since the work is generally labour-intensive and some of the anticipated replication of tests was not realized. Panel construction, including cutting and washing the reinforcing rods, preparing mesh, lay-up, and mortaring, consumed much of the available time. Cutting up of large panels by a diamond saw, testing the many flexure prism specimens, compression cubes and prism pieces, the

necessary experimenting with tensile gripping devices and specimen shapes, and the modification of a standard extensometer to measure the strain also consumed much of the available time.

Ten ferrocement test panels, 36 x 36 x 1 in., were made in an upright position with mortaring from both sides. The strength of the mortar was determined at 7 and 28 days from 2-in. compression cubes and at 28 days from 1.575 x 1.575 x 6.3 in. flexure prisms. The tensile strengths of reinforcing rod and mesh specimens were also determined. Selected panels, containing two layers and three layers of 1/2 in.-19 gauge galvanized hardware cloth on each side of 0.225 in. high-tensile double-drawn rod spaced on 2-in. centres in both directions, were cut into test specimens 6 in. wide and of various lengths, i.e., 12, 18, 24, and 36 in. The specimens were used for tensile and flexure tests. The tensile tests presented serious problems of gripping and shaping and the test results obtained are not especially useful. A number of flexure tests were made in which the deflections under load at the third-point load and midspan locations were reported. The strain was measured by a linear variable differential transformer extensometer adapted to a 6-in. gauge length and recorded graphically. The load at the first visible crack and maximum load held were recorded. The modulus of rupture and values of effective elastic moduli for 12 specimens from panels of two kinds of construction were calculated on the basis of the radius of curvature of a beam under load and on the basis of the unit fibre stress/unit fibre strain relationship at two load levels, viz., load at first visible crack,  $P_{fvc}$ , and 400 lb or  $\sim 0.5 P_{fvc}$ . The effective modulus of elasticity values obtained from the unit stress/strain relationship are more conservative than those obtained from the beam curvature formula and range from  $0.6 \times 10^6$  to  $1.2 \times 10^6$  psi for the ferrocement panels tested.

The distances of the various layers of mesh and rod reinforcement in each of the panel specimens from the tension-side surfaces were measured at the midspan and third-point locations. The average values are presented for future use in the development of a mathematical model.

Specimens from the same panels were subjected to a 500 lb load (a maximum fibre stress of about 1500 psi) 10 times to ascertain any "hysteresis effect" from multiple loading. The tangent modulus of elasticity at 500 lb for the second (and subsequent) cycle(s) of loading was much higher than the modulus obtained from the first loading cycle. No "hysteresis effect" or strength degradation was experienced in the 10 cycles of loading to a load equal to about half of the load for first visible crack.

The relationship of seawater corrosion and width of cracks has been examined. No serious amount of corrosion of the 1/2-19 gauge galvanized hardware cloth was observed after two months submerged exposure of specimens containing cracks as wide as 0.6 mm on the surface.

Painted specimens previously exposed in seawater at mean tide and below low tide for 84 days, mid-February to mid-May, were exposed for another 150 days, end of May to end of October. No biological growths, except for slime, attached themselves to the specimens coated with an ethyl silicate zinc-rich paint and with a vinyl resin-base antifouling paint. Barnacles had attached themselves to and severely damaged the specimens coated with a polyester resin vehicle. The other specimens with top coats of chlorinated rubber-based, polyvinyl chloride-based, pigmented epoxy resin-based, and polyamide resin paints were undamaged by the attached barnacles. Some paint damage would almost surely result from a hull scraping job which removed the barnacle pads as well as the shell.

The ferrocement bibliography has been updated and included as an Appendix to this study. Additions to the ferrocement bibliography have not been numerous. An Introduction to Design for Ferrocement Vessels, prepared by Dr. Gordon W. Bigg for the Fisheries Service, Environment Canada, is an especially useful review of the ferrocement technology and engineering design data. The preparation of the References on Ferrocement in the Marine Environment, by the Ferrocement Task Group HS-6-4 of the Society of Naval Architects and Marine Engineers, is also a useful addition.

### C. TEST PROGRAM.

#### 1. Preparation of Test Panels.

Part of the whole program was planned to provide strength data which could be eventually used in the development of a mathematical model. In all, ten 36 x 36-inch test panels were made. As in most of the earlier work reported, the panels were made free-standing, without a mould, to simulate the method of plastering or mortaring used by many boat-builders. The use of a form mould allows the mortar to be "floated" through the several layers of mesh with relative ease by means of a vibrating trowel or vibrating mould. Vibration has been found to be almost impossible to use effectively in the free-standing mould. (The use of an orbital sander attached to a trowel referred to recently may be a more effective yet gentler means of vibration than the pneumatic device used in tests here.) The free-standing mould does, however, permit plastering from both sides of the panel. Panel springiness does not allow the same panel flatness, uniformity of panel thickness, or uniformity of mortar cover over the mesh reinforcement that is possible in a form mould vibrated and trowelled in a horizontal position.

As before, the 38 x 38 in. panel frames of 2 x 4 in. wood were used for all the test panels. The reinforcing rods were inserted into holes spaced at 2-inch intervals along each side of the frame.

Layers of mesh reinforcement, 36 x 36-in. squares, were laid on both sides of the rods and wired to the rod intersections on 6-inch centres. Each layer of mesh was oriented so that the direction of the mesh wires provided an alternate transverse/lengthwise pattern across the panel cross-section. (Several of the panels were discovered to not conform to this pattern and were kept for non-critical tests.)

The steel reinforcement for all panels was as follows:

- Rods - 0.225 high-tensile double-drawn rods.
- Mesh - 1/2-19 gauge galvanized welded hardware cloth.
- Tie wire - Soft galvanized 18 gauge wire.

The average tensile strength properties of the rod material, obtained on four tests, are as follows:

Diameter, in.	0.223
Breaking Strength, lb	3,360
U.T.S., psi	86,000
Y.P. 0.2%, psi (dividers only)	72,000
Elongation, % in 10 in.	6.5

The average tensile strength properties of the wire mesh, based on one- and two-wire lengthwise and transverse specimens from three mesh samples, are as follows:

Diameter (stripped free of zinc), in.	0.038
Breaking Strength, lb	63
U.T.S., psi	55,000
Y.P. (Approx), psi	44,000

The specific surface of the mesh reinforcement, i.e., the total surface area of the wire in contact with the mortar divided by the volume of the composite, is about  $7.1 \text{ in.}^{-1}$  for all panels. The specific surface is calculated by

$$K = \frac{2\pi dn}{at}, \text{ where}$$

d = diam of wire (galvanized diameter)

n = number of layers

a = wire spacing

t = thickness of specimen

In calculating the specific surface for panel specimens reinforced with rods and mesh, the thickness t is considered to be only that portion of the specimen containing the mesh, i.e., t is the panel specimen thickness less the thickness of the rod section (2 x 0.225 in.) and the thickness of the mortar cover.



The panel construction details are summarized in Table 3.

The mortar mix for each panel was prepared in a standardized manner as follows:

Type II Cement (Ocean Cement Co.),	40 lb
Dry Mortar Sand (-8 mesh, Ocean Cement Co.),	80 lb
Water (containing 300 ppm chromium trioxide),	16 lb

A water/cement ration of 0.4 was attempted but up to two pounds of extra water was always required to get a workable mix, a slump of 2 1/2 to 3 in. In spite of the standardized procedures used, the workability varied from panel to panel, some difficulty being experienced in achieving full penetration through the panel mesh. Variation in the fineness of the sand from bag to bag is a possible cause of the variable workability.

Nine 2-inch cubes for 7-day, 28-day and spare compression tests (ASTM C109) were made from the mortar of each panel batch. Three 1.575 x 1.575 x 6.3 in. prism test specimens (ASTM C348) for 28-day flexure tests were made from each batch in the collapsible steel mould assembly prepared for this purpose. The broken halves of the beam specimens were used for 28-day compression tests (ASTM C349). The specimens were wrapped in wet paper towels, placed in a plastic bag, and stored at room temperature until tested. The test panels were stored in a vertical position under plastic sheeting and were wetted regularly during the 28-day cure period.

The average compression and flexural strengths of the mortars of the 10 panels are as follows:

Compression Strength (C109 and C349)

2-in. cubes	- 7 days 5400 psi
	- 28 days 7700 psi
1.575 x 1.575 in. prisms	- 28 days 10,000 psi

Flexural Strength (C348)

1.575 x 1.575 x 6.3 in. prisms	- 28 days 1350 psi
--------------------------------	--------------------

The individual test values for all specimens from 10 panels are provided in Tables 4 and 5 to show the range.

Tensile and flexural testing was mainly confined to two test panels, 207 and 208, respectively containing two and three layers of 1/2-19

gauge galvanized welded hardware cloth on each side of the 0.225 in. high tensile rods on two-inch centres.

The panels were sawn with a diamond masonry saw according to the pattern shown in Figure 1 to yield a series of test specimens six inches wide. The cutting of each panel yielded two specimens 12 in. long for tensile tests and four specimens 18 in. long, two specimens 24 in. long, and two specimens 36 in. long for flexure tests. The variety of lengths of the flexure test specimens was made to indicate the significance of rod/mortar bond length on flexural strength. (In practice, the transverse and lengthwise rods may be welded together at a number of intersections to provide a keying action between the rod and mortar.)

## 2. Tensile Testing.

Some experimentation was undertaken to develop a suitable method of tensile testing specimens from ferrocement panels. The testing of specimens from panels containing only mesh presents no really difficult problems. However, specimens from panels containing longitudinal rod reinforcement which is not welded to the transverse rod reinforcement is much more difficult.

Several requirements must be met:

- The specimen should be able to be tested in the available standard tensile testing equipment. (The equipment available in this laboratory is a Tinius Olsen Universal Testing Machine Model "Super L" of 60,000 lb capacity in three ranges, 0-1,200 lb, 0-12,000 lb, and 0-60,000 lb, with a maximum space between the cross-heads of 24 in.)
- The test results obtained from a test specimen must reasonably represent the strength of the material in the panel (hull or deck).
- The shape of the test specimen should not be difficult to generate from a panel and should not be cast separately.
- The shape must minimize stress concentrations.
- The loading attachments must be able to grip the specimen in such a way that the tensile breaking load can be applied without the imposition of bending loads. For example, cast-on epoxy wedges fitted into the cross-head cavities would not be an acceptable mechanism.

The test program examined several means of gripping the tensile test specimens using 4 x 12 x 1 in. specimens before using the six-

inch wide specimens from 207 and 208. The types of specimen and gripping attachments are shown in Figure 2. The following tests were undertaken:

- (a) A 4 x 12 x 1 in. specimen cut from earlier panels made with 0.225 in. high-tensile reinforcing rods spaced on 2-in. centres in both directions and two layers of 1/2-19 gauge galvanized hardware cloth on each side of the rod reinforcement was tested by tightly clamping the specimen between two pairs of grips over a 4-inch length at each end. The grips were made from steel checker floor plates which provided gripping points under the high clamping pressure (Figure 2.a). It was not possible to break the specimen because of slippage between specimens and grip plates.
- (b) A 4 x 12 x 1 in. specimen similar to that described in (a) was prepared by coating the end portions with a thick layer of an epoxy/sand mixture into which the gripping points of the checker plate grips were impressed. The specimen broke 4 in. from one end at a load of 4,360 lb. This load was held by 35 wires, the 4-inch rod/mortar bond length for two rods, and the tensile strength of the mortar. (If the total load carrying capacity of the wires is about  $65 \times 35 = 2,275$  lb and the mortar is 0.1 x compression strength = 2,400 lb, then the rod/mortar bond has contributed little to the composite strength in this test specimen.)
- (c) A 4 x 12 x 1 in. specimen similar to that in (b) was prepared to partially simulate the effect of a very long rod/mortar bond length or of anchoring the rods by welds to transverse rods or to end connections. A bar 1/4 x 4 in. was plug-welded to the tips of the two reinforcing rods exposed at each end of the specimen. The loading attachment, described in (b), was unable to break the specimen.
- (d) A 4 x 12 x 1 in. specimen was gripped by two bars on each end of the specimen. The bars were attached by two tightened bolts per end through 1/2-in. holes drilled through the specimen. A 1/2-in. hole was also drilled at mid-length and a half-hole at each side at mid-length to reduce the section of the specimen (Figure 2.b). In spite of this reduction, the specimen broke at one of the attachment holes where the stress concentration is undoubtedly greatest.
- (e) Specimens, 6 x 18 x 1 in., were prepared from Panels 207 and 208 with reduced sections over a 6-in. gauge length. The panels were reinforced with 0.225 in. high-

tensile double-drawn rod on 2-in. spacing in both directions. Panel 207 had two layers of 1/2-19 ga. galvanized hardware cloth on each side. Panel 208 had three layers. The specimens were prepared with a masonry drill and diamond saw to a reduced section 2-in. wide over a 6-inch gauge length. The shoulders were cut at a small angle to accommodate a special set of grips fabricated for these specimens (Figure 2.c). The fillets between shoulder and reduced section were made by drilling holes, 1/2-in. diam, at each of four locations prior to the diamond sawing operation. Each specimen contained only one longitudinal 0.225 in. rod in the centre of the specimen. Specimen 207-3 had 16 lengthwise wires, 208-3 had 23 wires.

The following strengths were obtained:

	<u>Load at first visible crack, lb</u>	<u>Max Load</u>
Specimen 207-3	1300	1420
Specimen 208-3	1450	1900

The load/strain curves, shown in Fig. 3 and 4, were obtained using a standard 2-in. gauge length extensometer adapted to a 6-in. extension. The modulus of elasticity for the two specimens from 207 and 208 are 1.10 and  $0.94 \times 10^6$  psi, respectively.

It is felt that the "in situ" strength of ferrocement material is not adequately appraised by any of the specimen shapes, attachments, and gripping arrangements used in this study. Each specimen was difficult to grip, difficult to prepare, subject to serious stress concentration effects, or failed to utilize the strength of the rod reinforcement.

### 3. Flexure Testing.

#### (a) Procedure and Test Results.

Flexure tests were performed on pairs of 18-, 24-, and 36-in. long x 6-in. wide test specimens to assess the bending properties of two lay-up constructions, viz., 2 layers of 1/2-19 gauge galvanized welded hardware cloth on each side of the 0.225 in. rods on 2-in. centres and 3 layers on each side of the rods and to assess the effect of specimen length, i.e., rod/mortar bond length on bending behaviour.

The flexure tests were performed on a span of 18 in. with third-point loading using a spherical loading head and rocker supports to accommodate any unevenness in the specimens. The deflection of the beam specimen was measured by dial gauges under each loading point and at mid-span. The strain in the tension side of the specimens was measured by means of a linear variable differential transformer extensometer (Tinius Olsen S1) and electronic recorder. The extensometer, with a standard 2-in. gauge length, was modified to extend over a 6-in. gauge length, the distance between the third-point loads.

The beam deflections at mid-span and at the third-point load locations were recorded for 100-lb increments of load. The first visible crack (fvc) and visible slipping of the reinforcing rod were also recorded. The mid-span deflection (D), the difference between mid-span and average of third-point deflections ( $\Delta D$ ), the tension-side fibre strain in./in., and the appearance of first visible cracking and rod slippage are provided in Table 6. The load/fibre strain curves for specimens from Panel 207 are reproduced in Figures 5 to 7 and from Panel 208 in Figures 8 to 10. Some of the curves show extensometer slippage.

An accurate knowledge of the location of the reinforcement within the panel is required for useful application of the flexural data for any mathematical model. The distance from the extreme tension surface of the centres of both lengthwise and transverse wires in each layer of mesh and of the lengthwise and transverse rods was measured at three locations: A, at one third-point load support; B, at centre load; and C, at the other third-point load support. The averages of the A, B, and C values are tabulated in Table 7.

The load, deflection, and strain values obtained were used to calculate the following:

- i. Modulus of rupture, i.e.,  $F = \frac{Mc}{I}$  at the maximum load held.\*
- ii. Effective modulus of elasticity in bending based on beam curvature formula  $\frac{1}{R} = \frac{M}{EI}$  at the load at first visible crack  $P_{fvc}$  and at 400 lb ( $\sim 0.5 P_{fvc}$ ).
- iii. Effective modulus of elasticity in bending,  $E = \frac{\sigma}{\epsilon}$ , based on fibre stress formula  $F = \frac{Mc}{I}$  at the load

\*No attempt has been made to determine the actual neutral axis and  $c$  is assumed to be  $t/2$ .

at first visible crack  $P_{fvc}$  and at 400 lb ( $\sim 0.5 P_{fvc}$ ).

(The values obtained are based on tangent slope at  $P_{fvc} \pm 100$  lb and  $400 \pm 100$  lb.)

The values for modulus of rupture, effective modulus of elasticity,  $E = \frac{RM}{I}$  and effective modulus of elasticity,  $E = \frac{\sigma}{\epsilon}$ , are provided in Tables 8, 9, and 10, respectively.

(b) Interpretation and Discussion.

The load/strain curves (Figures 5 to 10) and the tabulated data (Tables 8, 9, and 10) are the basis of the following observations:

i. Modulus of Rupture.

Although the differences are not generally great, the maximum load held and the modulus of rupture value increases with the length of the specimen. The average modulus of rupture values for 18-in., 24-in., and 36-in. specimens from Panel 207 (two layers of 1/2 in.-19 ga. mesh on each side) are 3500, 3950, and 4400 psi, respectively, and from Panel 208 (three layers of 1/2 in.-19 ga. mesh on each side) are 3600, 4350, and 4400 psi, respectively. The greater rod/mortar bond area of the longer specimens is assumed to be responsible for the positive relationship between modulus of rupture and specimen length. The smaller difference in modulus values between the 24-in. and 36-in. specimens than that between the 18-in. and 24-in. specimens suggests that tests on specimens longer than 36 in. may not have given much higher values of the modulus of rupture.

ii. Effective Modulus of Elasticity.

The effective modulus of elasticity of the flexure specimens at the load at the first visible crack and at 400 lb has been obtained by two methods.

The calculation of the effective elastic modulus by the curvature method is based on the fact that the curvature  $1/R$  of a simply supported, homogeneous, elastic beam, constant in cross-section (i.e., constant  $E$  and  $I$ ), and under a load (which does not exceed the elastic limit) varies directly with the moment and is a constant value for all sections between the equal

loads applied an equal distance from the supports,  
i.e.,  $\frac{1}{R} = \frac{M}{EI}$ .

The value of R has been calculated from the difference  $\Delta D$  in the dial gauge reading at mid-span and the average of the dial gauge readings at the third-points.

The average values of effective modulus of elasticity at the load at first visible crack ( $P_{fvc}$ ) calculated by the beam curvature method are  $1.62 \times 10^6$  psi for specimens from Panel 207 and  $1.96 \times 10^6$  psi for specimens from Panel 208. The tabulated values are provided in Table 9. The values at 400 lb ( $\sim 0.5 P_{fvc}$ ) are higher and more erratic. The wide range of values is due to the inherent variable nature and non-homogeneity of a composite material such as ferrocement and to variations in the geometry within the specimen and from specimen to specimen. At low loads, even 400 lb, the value of  $\Delta D$  is small resulting in high and possibly erroneous values of R and E.

The effective moduli of elasticity have been calculated for the 18-, 24-, and 36-in. specimens from Panels 207 and 208 according to

$$E = \frac{\sigma}{\epsilon}$$

where  $\sigma$  = unit tensile fibre stress in the beam and  $\epsilon$  = the unit tensile fibre strain determined by the strain gauge between the third-point loads at the load at first visible  $P_{fvc}$  and 400 lb. The moduli have been calculated on the basis of the tangent slope at  $P_{fvc}$  and 400 lb (actually the slope at  $P_{fvc} \pm 100$  lb and  $400 \pm 100$  lb, respectively). The average moduli calculated for  $P_{fvc} \pm 100$  lb and  $400 \pm 100$  lb are  $0.92 \times 10^6$  and  $1.27 \times 10^6$ , respectively, for specimens from Panel 207 and  $0.74 \times 10^6$  and  $1.24 \times 10^6$ , respectively, for specimens from Panel 208. The tabulated values are provided in Table 10.

#### 4. Tests to Establish Stress/Strain Hysteresis Effect.

Two 18 x 6 x 1 in. specimens 207-2 and 208-2 were tested in flexure to establish the stress/strain characteristics under repeated loading in flexure. The flexure test set-up used was the same used for the other flexure tests except that only the mid-span deflection was measured by means of a dial gauge. The modified 6-in. strain gauge was attached to the tension side of the specimen.

The specimen 207-2 was loaded to 500 lb (a level below the probable appearance of the first visible crack) in about 50 seconds. The tension-side strain was recorded on the stress-strain recorder. The load was removed and reapplied in a similar manner for a total of 10 load cycles, the load/strain being recorded for each cycle. The repeated load/strain cycles on an expanded load scale are shown in Figure 11.

The specimen 208-2 was similarly loaded to 500 lb. The beam mid-span deflection at 100-lb increments was recorded and the tension-side strain was recorded on the load/strain recorder for the 10 load cycles. The deflections are presented in Table 11 and the load/strain curves are shown in Figure 12.

The curves indicate that plastic strains of about 0.0005 in./in. for specimen 207-2 and 0.0003 in./in. for specimen 208-2 result from the first load cycle. No further plastic strain was encountered in subsequent load cycling.

The effective moduli of elasticity calculated from the flexural test load strain results on the first load cycle (tangent at 500 lb load) and on subsequent load cycles for specimens 207-2 and 208-2 are as follows:

	<u>First Load Cycle</u>	<u>Subsequent Load Cycles</u>
207-2	$0.86 \times 10^6$ psi	$1.88 \times 10^6$ psi
208-2	$1.41 \times 10^6$ psi	$2.82 \times 10^6$ psi

The "breaks" in the load/strain curve (first load cycle only) at a load of 100 to 125 lb are more pronounced than in earlier curves on a more compressed load scale.

#### 5. Tests to Examine Critical Crack Width.

Several investigators have concerned themselves with cracking under load related to steel dispersion, water seepage through the panel (hull), and corrosion of the reinforcement. The tests conducted in this study were initiated to shed further light on the relationship between mortar cracking and mesh reinforcement corrosion.

Three pairs of 6 x 18 x 1 in. and one pair of 6 x 36 x 1 in. specimens were selected from Panels 201 and 202 for testing under third point flexural loading. The specimens of each pair were loaded in as similar manner as possible. The loading was stopped on the basis of the appearance of tension side cracking and equal strain as indicated by the load/strain curve obtained with the 6-in. strain gauge already described. The deflections at the load points and at mid-span were also recorded and are presented in Table 12.



The widths of the main cracks in one specimen of each pair were measured by means of a calibrated microscope and are presented in Table 13.

These four specimens were immersed in seawater for two months, removed and allowed to dry in air. Two of the exposed specimens, 201C and 201G, and one of the unexposed specimens, 201A, were retested in flexure. The load/strain curves were compared. Finally, the mortar or the tensile side of the specimens exposed in seawater was chipped away to reveal the condition of the mesh and rod reinforcement. Any evidence of rust staining of the wire was noted. Some of the exposed wire was checked with 35 percent cupric sulphate solution for the absence of zinc coating.

The load/strain curve for the flexure test on specimen 201C after the seawater exposure did not differ greatly from the curve obtained before the exposure. The load/strain curve for specimen 201G was unsatisfactory because of strain gauge slippage. The load held by the unexposed specimen 201A on retest was considerably lower than the load held by the original test.

Specimen 201C, containing cracks up to 0.1 mm wide, showed no rusting of the wires. Specimen 201F showed no evidence of corrosion on wires under a crack 0.2 mm wide but local rust stains were observed on three wires under a 0.4 mm wide crack. No rust stains were observed on the wires of 201G under three cracks 0.4 to 0.6 mm wide. Many of the wires had necked and broken. The copper sulphate test on the necked wires and on wires from other locations showed that the zinc coating had flaked off in some areas. The mesh layer examined was about 0.1 in. below the specimen surface in all cases, i.e., a mortar cover of about 0.1 in.

The tests performed do not permit absolute conclusions to be drawn. However, no serious corrosion of the mesh has occurred even in cracks as wide as 0.6 mm after an exposure in seawater of two months. Tidal conditions, wetting and drying, working of the crack under stress might aggravate the corrosion condition.

## 6. Seawater Exposure Tests on Painted Specimens.

Ferrocement panels had been prepared and painted with 12 coating systems for exposure to a marine environment as reported in Vol III of this series. The complete list and description of the paint systems used are provided in Table 14. The specimens, previously exposed and rated, were returned to the seawater environment for a further exposure period.

### (a) Marine Tidal Exposure.

Duplicate 3 x 3-in. specimens had been exposed for 84 days at the Vancouver Kitsilano Station of the Canadian Coast Guard.

One set was installed below low low tide and one at about mean tide between mid-February and mid-May 1972. The condition of each coating after 84 days was rated and reported. The specimens were covered with a coating of slime but were otherwise visibly unimpaired.

The two 12-specimen lots were re-installed at mean tide and low-low tide near the end of May and were exposed for an additional 150 days. The general appearance of the coatings was good. However, an abundant crop of small barnacles had attached themselves to all specimens except those in the upper left-hand corner, Figures 13, 14, and 15. The corner specimen is coated with an inorganic two-component self-curing ethyl silicate zinc-rich paint used as primer and top coat. The adjacent blue specimen has a two-component clear epoxy finish primer with two top coats of vinyl resin base anti-fouling paint.

The specimens were scraped free of the barnacle growth and re-examined. Scraping easily removed the barnacle shells but the base plates of the barnacles remained attached to the paint substrate. Casual visual examination revealed no apparent impairment of the paint coatings, Figures 16 and 17. Close inspection under the microscope, however, showed that the base plates of the barnacles had removed the paint to bare mortar from the specimens coated with the highly-modified polyester resin vehicle containing metal and oxide fillers. The barnacles did not attack the other coatings but scraping to remove the base plates of the barnacles caused some damage to the paint coating. The specimens with top coats of two-component polyamide resin appeared to suffer least damage from the barnacles. The appraisal of the 12 systems is presented in Table 15. Figures 18 and 19 show two typical conditions of the paint at growth locations.

In summary, the specimen coated with the ethyl silicate zinc rich paint and the specimen coated with the vinyl resin base anti-fouling paint were free of barnacles, the specimens coated with a chemical-cured polyamide resin had barnacle attachments which separated easily and with little damage to the paint, the chlorinated rubber-based and polyvinyl paints had barnacle attachments which adhered more firmly. Hull scraping to remove the barnacle attachment pads completely would almost surely damage the paints.

(b) Laboratory and Seawater Exposure.

Duplicate specimens, already described in Vol III of this series, received 600 exposure cycles, i.e., one hour of wetting in filtered seawater and three hours of air-drying in front of a fan. The specimens were re-exposed for another 2,000 cycles and re-rated. There was no visible change in the condition of the paint specimens.

D. GAPS IN THE TECHNOLOGY OF FERROCEMENT.

Many gaps still exist in the technology of ferrocement. Many areas have been subjected to fairly intensive studies, even though uncoordinated, whereas other areas have been hardly touched. The Society of Naval Architects and Marine Engineers Task Group HS-6-4 has presented proposals for 10 areas requiring further study to the Hull Structures Committee. These are:

1. Static tests - to demonstrate reproducibility of mechanical test data in tension, shear, flexure, and compression.
2. Specific surface - to study the effect of specific surface on the mechanical properties of ferrocement in tension, shear, flexure, and compression.
3. Comparison of mesh configuration - to study the effect of mesh configuration on the mechanical properties of ferrocement in tension, shear, flexure, and compression.
4. Reinforcement - to evaluate the effectiveness of rod type reinforcement on ferrocement.
5. Creep tests - to study the creep behaviour of a typical ferrocement composition due to a constant load on a flexure panel.
6. Impact tests - to develop a standard test for a blunt object impact to assess the effect of specific surface of reinforcement on the impact resistance of ferrocement.
7. Impact tests - to compare the relative impact strength of typical ferrocement specimens with competitive hull materials, e.g., wood (plywood), glass fibre reinforced plastic, steel, (and aluminum).
8. Service experience - to compile a problem profile of ferrocement construction on vessels already constructed with a view to guiding further investigation into those areas shown to be of significance.

9. Durability, crevice corrosion - to determine the corrosivity of the reinforcement in ferrocement specimens with cracks of various widths.

To these should be added:

10. Hydrostatic tests - to study the behaviour of ferrocement under hydrostatic loadings from the head of water and dynamic heads.
11. Fatigue tests - to study the behaviour of ferrocement under cyclic flexure loads of constant magnitude rather than of constant displacement.
12. Non-destructive quality control - to develop sonic, ultrasonic, and other tests which can detect incomplete penetration of the mortar and other defects before the mortar has set.

It is felt that workers in the field of ferrocement should coordinate their efforts through a coordinating body such as SNAME to avoid duplication of efforts.

#### E. REVIEW OF LITERATURE.

Several technical papers and reports have been examined and added to the Bibliography maintained in these studies over the past several years.

The work of Christensen and Williamson on the galvanic cell problem in ferrocement (item 90) was omitted from the last report.

Tancreto and Haynes (item 91) have tested ferrocement panels reinforced with plain steel woven wire mesh (from 2 x 2 to 14 x 14 wires per inch), subjected to flexural loads to determine first cracking, visible cracking, and ultimate strength properties. They rated meshes of various mesh size and wire diameter, and compare with chicken wire, on the basis of mechanical properties of test panels containing no rod reinforcement, the workability of the fabrication process, and the cost of the reinforcement. The mechanical properties included the strength at first cracking, strength at first visible cracking, ultimate strength and toughness, and crack control. Workability includes the ease with which mortar penetrates the reinforcement materials. The authors conclude that the best reinforcement material is 4 x 4 mesh of 0.025 in. diameter wire. Chicken wire on 0.25 in. rods on six inch centres in both directions ranked third on a 1 to 5 ranking grade for the nine systems.

Bigg (item 92) has provided a significant contribution to the ferrocement technology with his survey and rationalization of ferrocement parameters and constants obtained from the abundant literature. He feels that this composite material, ferrocement, can be characterized by a knowledge of:

- (1) Specific surface of the mesh.
- (2) Reinforcement factor of the mesh and rod.
- (3) Ultimate compressive strength of the mortar at 28 days.
- (4) Precise geometrical description of the reinforcement configuration.
- (5) Composite stress and stiffness to first crack of a corrosive size in tension, shear, and bending.

Bigg emphasizes, as many have before him, that the development of ferrocement technology is handicapped by the lack of appropriate testing standards which may be used by the many workers in the field of ferrocement research and testing. This lack of standards has made comparisons of published test results difficult or impossible.

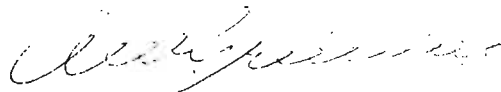
The United Nations study by Sutherland (item 93) is "designed to serve as a guide to technical assistance by UNIDO in this field (ferrocement shipbuilding) and to support its activities". The study provides cost data on materials and labour, design criteria, construction details, American Bureau of Shipping and Ferro-Cement Limited guidelines for design and construction of ferro-cement vessels, and the results of drop and fire tests on a 27-ft launch hull.

The report for the National Academy of Sciences (item 94) was prepared as part of "its continuing systematic search for, and assessment of, developments in fields of science and technology that may bear particular relevance to the solution of specific problems in developing countries". The study is perhaps unique in ferrocement literature in that equal attention is given to applications of ferrocement for boatbuilding, food-storage facilities, food-processing equipment, and low cost roofing. The advisory panel concludes that the potential of ferrocement in developing countries and its likely effect on their economies are much greater than previously thought. The panel recommended the establishment of an international service to collect and disseminate information on ferrocement science which could prevent unnecessary duplication of research and development and ensure that developing countries are fully informed of relevant experience with ferrocement. The information service should: (1) maintain an information bank and inquiry referral service, (2) disseminate information on research and development efforts and on advances in ferrocement technology and experiences in applying it (to specific products), and (3) help developing countries identify experienced

ferrocement companies and consultants, especially those with experience in developing countries.

The Task Group HS-6-4 (Ferrocement) of Panel HS-6 (Materials) Hull Structure Committee of the Society of Naval Architects and Marine Engineers has compiled some 270 technical references (item 95) on ferrocement and concrete as a construction and fabrication material for boats, barges, vehicles and other structures which operate in a marine environment.

The work done by B.C. Research for the Fisheries Service, Department of the Environment, Ottawa, from 1969 to 1972, has not been previously annotated and is now included herein as items 96 to 99.



A.W. Greenius  
Division of Engineering



R.E.W. Lake  
Head, Division of Applied Physics

AWG/mc

REFERENCES.

1. Kelly, A.M. and T.W. Mouat, Ferro-Cement as a Fishing Vessel Construction Material, 1969, pp 75, published as part of Project Report No. 42, Ferro-Cement for Canadian Fishing Vessels, edit. W.G. Scott, Industrial Development Branch, Fisheries Service, Canada Department of the Environment, Ottawa, Aug. 1971.
2. Greenius, A.W., The Development of Ferro-Cement for Fishing Vessel Construction, March 31, 1970, pp 61, and Technical Supplement by A.W. Greenius and J.D. Smith, May 31, 1970, pp 58, published as part of Project Report No. 42, edit. W.G. Scott, Industrial Development Branch, Fisheries Service, Canada Department of the Environment, Ottawa, Aug. 1971.
3. Greenius, A.W. and J.D. Smith, Ferro-Cement for Fishing Vessel Construction II, June 1971, pp 113, published as Project Report No. 48, Ferro-Cement for Canadian Fishing Vessels, Vol 2, Industrial Development Branch, Fisheries Service, Canada Department of the Environment, Ottawa, Jan. 1972.
4. Greenius, A.W., Ferrocement for Fishing Vessel Construction III, pp 54, June 1972, not yet published.





	Author - Affiliation	Title	Journal and Citation	Narrative	Tables	Dwgs. Figs.	Scale Dwgs.	Performance	Photographs	Costs	Refs.
97	Greenius, A.W. and J.D. Smith	ibid. Technical Supplement, pp 58, May 31, 1970.	ibid.	x	x	x		x	x		x
98	Greenius, A.W. and J.D. Smith	The Development of Ferro- Cement for Fishing Vessel Construction II, pp 113, May 31, 1971.	Ferro-Cement for Canadian Fishing Vessels, Project Report No. 48, Industrial Development Branch, Fisheries Service, Department of the Environment, Ottawa, Jan. 1972.	x	x	x		x	x		x
99	Greenius, A.W.	Ferrocement for Fishing Vessel Construction III, pp 54, June 1972.	Not yet published for distribution.	x	x	x		x	x		x

TABLE 1. TENSILE STRENGTH OF REINFORCING ROD.

Sample No.	Diam in.	U.T.S. psi	0.2% Y.P. psi*	Elong. % in 10 in.
1	0.223	85,500	74,000	8.5
2	0.223	86,600	74,000	5.2
3	0.223	85,000	71,500	5.0
4	0.223	86,400	69,000	7.4
Aver.		86,000	72,000	6.5

\*By divider method only.

TABLE 2. TENSILE STRENGTH OF 1/2-19 ga. GALVANIZED MESH.

Sample No.	Specimen	Breaking Strength, lb			
		Lengthwise Wire		Transverse Wire	
1	1-wire	68	68	62	62
	2-wire	128	64	125	62
2	1-wire	58	58	60	60
	2-wire	108	54	110	55
3	1-wire	70	70	70	70
	2-wire	140	70	132	66
Average		64		63	

TABLE 3. PANEL CONSTRUCTION DETAILS

Panel No.	Description
201	} 2 layers of 1/2-19 ga. galvanized hardware cloth. 1 layer 0.225-in. high-tensile rods at 2-in. spacing. 1 layer 0.225-in. high-tensile rods at 2-in. spacing. 2 layers of 1/2-19 ga. galvanized hardware cloth.
202	
207*	
210	
203	} 3 layers of 1/2-19 ga. galvanized hardware cloth. 1 layer 0.225-in. high-tensile rods at 2-in. spacing. 1 layer 0.225-in. high-tensile rods at 2-in. spacing. 3 layers of 1/2-19 ga. galvanized hardware cloth. 208* 209
204	
205	
206	
208*	
209	

\*The specific surface for Panels 207 and 208 =  $\sim 7.1 \text{ in.}^{-1}$

(The specific surface  $K = \frac{2\pi dn}{at}$ , where  $d$  = wire diam,  $n$  = number of layers of mesh,  $a$  = wire spacing, and  $t$  = thickness of specimen portion containing the mesh only, i.e., full thickness of panel - (twice rod diam + thickness of surface mortar).)

$$K_{207} = \frac{2\pi(0.043)2}{0.5(0.15)} = 7.2 \text{ in.}^{-1}$$

$$K_{208} = \frac{2\pi(0.043)3}{0.5(0.23)} = 7.1 \text{ in.}^{-1}$$

TABLE 4. COMPRESSION STRENGTH OF MORTAR

Panel No.	Compression Strength (Sc), psi			
	2-in. cubes		1.575 x 1.575 in. prism	
	7-day	28-day	28-day	
201	5,700	8,200	8,200	8,500
	5,900	9,600	7,700	8,400
	5,200	6,800	9,000	9,900
Average	5,600	8,200	8,600	
202	3,600	6,800	7,500	8,400
	3,900	5,800	7,800	8,100
	3,700	6,000	8,800	8,800
Average	3,700	6,200	8,200	
203	4,300	8,100	10,000	9,600
	4,800	6,500	9,400	9,700
	5,000	7,300	10,800	-
Average	4,700	7,300	9,900	
204	5,200	7,800	10,000	10,000
	5,200	8,000	10,400	10,500
	6,000	6,800	11,600	11,100
Average	5,500	7,500	10,600	
205	5,300	6,700	10,500	10,000
	4,900	7,100	8,500	10,200
	5,800	7,400	9,600	11,300
Average	5,300	7,100	10,000	
206	4,800	7,700	8,500	9,900
	5,100	8,100	10,300	10,400
	5,600	8,700	10,200	10,300
Average	5,200	8,200	9,900	

TABLE 4. Continued.

Panel No.	Compression Strength (Sc), psi			
	2-in. cubes		1.575 x 1.575 in. prism	
	7-day	28-day	28-day	
207	4,700	8,200	10,900	10,200
	5,500	-	11,200	10,000
	5,700	8,600	10,100	10,100
Average	5,300	8,400	10,400	
208	6,600	7,800	12,300	12,000
	5,800	7,700	12,400	11,700
	6,500	8,800	11,000	10,200
Average	6,300	8,100	11,600	
209	6,600	7,800	10,900	11,700
	6,600	7,700	11,500	11,100
	5,600	8,400	11,500	11,800
Average	6,300	8,000	11,400	
210	6,100	7,100	11,000	9,700
	6,500	8,900	11,200	9,700
	5,500	7,500	9,700	-
Average	6,000	7,800	10,300	
Average 10 panels	5,390	7,680	10,090	
Average exluding 203	5,700	7,912	10,350	

TABLE 5. FLEXURAL STRENGTH OF MORTAR.  
 (Prism specimen 1.575 x 1.575 x 6.3 in.)  
 (28-day curve)

Panel No.	Maximum Applied Load (P), pounds	Flexural Strength (S) S = 1.8 P, psi
201	630	1135
	620	1120
	637	1150
Average		1135
202	664	1195
	650	1170
	640	1155
Average		1173
203	830	1495
	890	1600
	-	-
Average		1548
204	810	1460
	700	1260
	960	1730
Average		1483
205	688	1240
	670	1210
	700	1260
Average		1237
206	720	1295
	710	1280
	700	1260
Average		1278
207	732	1320
	718	1295
	820	1475
Average		1363
208	806	1450
	737	1330
	752	1350
Average		1377
209	744	1340
	788	1420
	828	1490
Average		1417
210	832	1500
	812	1480
	-	-
Average		1490
Average 10 panels		1350

TABLE 6. LOAD vs. MIDSPAN DEFLECTION,  $\Delta D$ , AND FIBRE STRAIN FOR SPECIMENS FROM PANELS 207 AND 208.

Load lb	Midspan Deflection D, 0.001 in.	$\Delta D$ 0.001 in.	Fibre Strain in./in.	Remarks
<u>Specimen 207-1 (18")</u>				
0	0	0		
100	7	0		
200	15	1		
300	25	2		
400	37	3.5	0.00053	
500	50	4.5		
600	66	7		
700	82	10.5		
800	98	12.5	0.00170	First visible crack
900	116	13.5		
1000	140	19		
1100	165	21		
1200	190	23		
1230	213	25		Visible slipping of rods.
<u>Specimen 207-4 (18")</u>				
0	0	0		
100	10	1.5		
200	21	3		
300	32	5		
400	45	5.5	0.00056	
500	57	9		
600	71	10		
700	90	13		
800	100	14.5	0.00148	First visible crack.
900	116	17		
1000	136	20		
1100	156	23.5		Visible slipping of rods.
<u>Specimen 207-5 (24")</u>				
0	0	0		
100	7	0		
200	15	0		
300	20	1.5		
400	38	4.5	0.00064	
500	53	7		
600	72	9.5		
700	91	12.5		
800	115	17.5	0.00217	First visible crack.
900	139	22.5		
1000	172	27.5		Visible slipping of rods.

TABLE 6. Continued.

Load lb	Midspan Deflection D, 0.001 in.	$\Delta D$ 0.001 in.	Fibre Strain in./in.	Remarks
<u>Specimen 207-6 (24")</u>				
0	0	0		
100	8	0		
200	17	0		
300	28	0.5		
400	40	1.5	0.00045	
500	55	3.5		
600	70	6		
700	86	8		
800	104	10		
940	129	14.5		
1000	142	15.5		
1100	166	20	0.00252	First visible crack.
1200	184	23		
1300	215	26.5		
1400	255	33.5		
<u>Specimen 207-7 (36")</u>				
0	0	0		
100	10	0		
200	20	0		
300	33	0.5		
400	47	1.5	0.00068	
500	63	4		
600	78	5		
700	96	6.5		
800	116	9.5		
900	143	13.5	0.00235	First visible crack.
1000	171	17		
1100	206			
<u>Specimen 207-8 (36")</u>				
0	0	0		
100	14	0		
200	27	2		
400	56	6.5	0.00088	
500	68	8.5		
600	83	11		
700	97	13.5		
800	110	15	0.00190	
900	125	18		
1000	140	21		
1100	156	23		



TABLE 6. Continued.

Load lb	Midspan Deflection D, 0.001 in.	$\Delta D$ 0.001 in.	Fibre Strain in./in.	Remarks
<u>Specimen 207-8 (36") - cont'd</u>				
1200	172	26		
1300	191	29.5		
1400	212	33		
1500	215	40		
1550	280	47.5		
<u>Specimen 208-1 (18")</u>				
0	0	0		
100	7	0		
200	18	0		
300	31	1		
400	42	2.5	0.00066	
500	56	3.5		
600	70	5		
700	83	6		
800	100	8.5		
900	118	10.5		
1000	138	12.5	0.00276	First visible crack.
1100	160	13.5		
1200	186	17		Visible slipping of rods.
<u>Specimen 208-4 (18")</u>				
0	0	0		
100	-	0		
200	-	0		
250	26	0		
400	44	2.5	0.00066	
500	55	3.5		
600	69	6		
700	80	6.5		
800	93	8		
900	112	10.5		
1000	129	14		
1100	143	14.5	0.00266	First visible crack.
1200	163	17		
1300	183	18.5		
1400	210	21.5		
1450	230	23		Visible slipping of rods.

TABLE 6. Continued.

Load lb	Midspan Deflection D, 0.001 in.	$\Delta D$ 0.001 in.	Fibre Strain in./in.	Remarks
<u>Specimen 208-5 (24")</u>				
0	0	0		
100	6	0		
200	22	0		
300	39	1.5		
400	55	4	0.00090	
500	72	10		
600	87	12.5		
700	102	-		
800	120	12.5		
900	140	13	0.00282	First visible crack.
1020	167	16.5		
1200	205	21		
1400	257	23.5		
1500	290	30.5		
1600	330	35		
1700	395	42		
<u>Specimen 208-6 (24")</u>				
0	0	0		
100	6	0		
200	17	0		
300	30	0		
400	41	1		
500	54	2.5		
600	67	4		
700	80	-		
800	95	5.5		
900	113	8		
1000	128	9	0.00060	First visible crack.
1100	151	13.5		
1280	170	15		
1400	220	19		
1500	251	21	0.00226	Visible slipping of rods.
1600	318	30		

TABLE 6. Continued.

Load lb	Midspan Deflection D, 0.001 in.	$\Delta D$ 0.001 in.	Fibre Strain in./in.	Remarks
<u>Specimen 208-7 (36")</u>				
0	0	0		
100	7	0		
200	20	0		
300	32	0		
400	43	0.5	0.00064	
500	56	1.5		
600	70	3.5		
700	85	5.0		
800	103	7.0	0.00152	First visible crack.
900	125	9.5		
1000	149	12		
1100	176	15		
1200	210	19.5		
1300	243	25		
1400	283	30		
<u>Specimen 208-8 (36")</u>				
0	0	0		
100	10	1		
200	24	3.5		
300	40	5		
400	55	7.5	0.00080	
500	67	8		
600	80	9.5		
700	97	13.5		
800	114	14.5		
900	133	17.5		
1000	156	23	0.00280	First visible crack.
1100	180	27		
1200	210	28.5		
1300	240	32		
1400	310	41		
1500	387	44		

TABLE 7. DISTANCE OF MESH WIRES AND RODS FROM TENSION SIDE OF FLEXURE SPECIMENS

(Distances in 0.01 in.)

Specimen No.	Mesh				Rods						Mesh				
	a	b	c	d	e	f	g	h	i	j	k	l	m	n	o
207-1	19	22	29	32	-	-	48	70	-	-	81	84	90	93	102
-4	8	11	15	18	-	-	33	55	-	-	69	72	77	80	99
-5	14	18	22	25	-	-	39	61	-	-	78	81	84	87	102
-6	8	11	17	20	-	-	36	58	-	-	74	77	81	84	95
-7	10	13	19	22	-	-	37	59	-	-	72	75	83	86	97
-8	12	15	19	22	-	-	39	61	-	-	77	80	85	88	93
-2	11	14	18	21	-	-	39	61	-	-	75	78	83	86	101
208-1	12	15	19	22	27	30	45	67	82	85	91	94	97	100	102
-4	11	14	18	21	25	28	42	64	78	81	86	89	94	97	105
-5	13	16	22	25	29	32	45	67	82	85	89	92	99	102	107
-6	8	11	17	20	24	27	42	64	75	78	82	85	91	94	104
-7	9	12	17	20	25	28	42	64	77	80	84	87	93	96	106
-8	9	12	17	20	25	28	42	64	77	80	84	87	93	96	99
-2	9	12	18	21	25	28	42	64	74	77	83	86	94	97	108

Where a, c, and e are distances of centre line of longitudinal wires of mesh layers 1,2, & 3 from surf.  
 b, d, and f " " " " " transverse " " " " 1,2, & 3 " "  
 g is distance " " " " longitudinal rod from surface.  
 h is " " " " transverse " " "  
 i, k, and m are distances " " " " longitudinal wires of mesh layers 4,5, and 6 from surf.  
 j, l, and n " " " " transverses " " " " 4,5, and 6 from surf.  
 o is distance of compression side surface from tension side surface i.e. the thickness of the specimen.

TABLE 8 MODULUS OF RUPTURE,  $F = \frac{Mc}{I}$  AT MAXIMUM LOAD  
(18-in span third - point loading).

Specimen No.	Specimen Length, in	Max. Load lb.	Modulus of Rupture, psi.
207-1	18	1230	3600
-4	18	1100	3400
Average		1165	3500
207-5	24	1030	3100
-6	24	1420	4800
Average		1225	3950
207-7	36	1100	3700
-8	36	1550	5100
Average		1325	4400
Average		1240	3950
208-1	18	1200	3300
-4	18	1450	3900
Average		1325	3600
208-5	24	1700	4000
-6	24	1600	4100
Average		1650	4350
208-7	36	1410	3900
-8	36	1500	4900
Average		1455	4400
Average		1480	4120

TABLE 9. EFFECTIVE MODULES OF ELASTICITY CALCULATED FROM BEAM CURVATURE  
 FORMULA  $\frac{I}{R} = \frac{M}{EI}$  FOR LOAD AT FIRST VISIBLE CRACK AND 400 LB(No.5FVC)  
 (18-in,span, third point loading)

Specimen No.	Length in.	Effective Modulus of Elasticity, psi	
		at First Visible crack	at 400 lb.load
207-1	18	$1.38 \times 10^6$	$2.95 \times 10^6$
-4	18	$1.76 \times 10^6$	$2.08 \times 10^6$
-5	24	$1.19 \times 10^6$	$2.32 \times 10^6$
-6	24	$1.76 \times 10^6$	$8.50 \times 10^6$
-7	36	$2.14 \times 10^6$	$8.25 \times 10^6$
-8	36	$1.52 \times 10^6$	$1.96 \times 10^6$
Average		$1.62 \times 10^6$	
208-1	18	$1.85 \times 10^6$	$3.85 \times 10^6$
-4	18	$1.75 \times 10^6$	$3.70 \times 10^6$
-5	24	$1.57 \times 10^6$	$1.35 \times 10^6$
-6	24	$2.70 \times 10^6$	$9.70 \times 10^6$
-7	36	$2.65 \times 10^6$	$18.50 \times 10^6$
-8	36	$1.27 \times 10^6$	$1.95 \times 10^6$
Average		$1.96 \times 10^6$	

TABLE 10. EFFECTIVE MODULUS OF ELASTICITY CALCULATED FROM  $E = \frac{\sigma}{\epsilon}$  and  
 $\Delta\sigma = \frac{\Delta Mc}{I}$  FIBRE STRESS FORMULA FOR LOAD AT FIRST  $\epsilon$  VISIBLE  
 CRACK AND 400 LB ( $\sim 5 P_{fvc}$ ) (18-in span, third point loading).

Specimen No.	Length In.	Effective Modulus of Elasticity, psi.	
		At First Visible Crack	at 400 lb. load.
207-1	18	$0.88 \times 10^6$	$1.19 \times 10^6$
-4	18	$1.18 \times 10^6$	$1.57 \times 10^6$
-5	24	$0.60 \times 10^6$	$1.03 \times 10^6$
-6	24	$0.82 \times 10^6$	$1.34 \times 10^6$
-7	36	$0.91 \times 10^6$	$1.31 \times 10^6$
-8	36	$1.14 \times 10^6$	$1.20 \times 10^6$
Average		$0.92 \times 10^6$	$1.27 \times 10^6$
208-1	18	$0.75 \times 10^6$	$1.24 \times 10^6$
-4	18	$0.79 \times 10^6$	$1.21 \times 10^6$
-5	24	$0.58 \times 10^6$	$0.94 \times 10^6$
-6	24	$0.74 \times 10^6$	$1.35 \times 10^6$
-7	36	$0.92 \times 10^6$	$1.42 \times 10^6$
-8	36	$0.66 \times 10^6$	$1.31 \times 10^6$
Average		$0.74 \times 10^6$	$1.24 \times 10^6$

Table 11. MIDSPAN DEFLECTION OF SPECIMEN 208-2 LOADED TO 500 LBS  
TEN TIMES. (Deflection, 0.001 in.)

Load Lb.	Midspan Deflection, 0.001 in. for Load Cycles 1 to 10										
	1	2	3	4	5	6	7	8	9	10	11
0	0	2	2	2	2	3	3	3	3.5	3.5	3
100	0	8	10	8	9	8	8	9	9	9	
200	14	16	18	18	17	17	18	17	18	18	
300	20	23	24	25	24	24	24	24	24	25	
400	25	30	31	31	31	31	31	31	32	31	
500	37	38	38	38	39	39	38	38	38	39	



TABLE 12. LOAD vs. MIDSPAN DEFLECTION,  $\Delta D$ , AND FIBRE STRAIN FOR SPECIMENS FROM PANELS 201 AND 202.

Load lb	Midspan Deflection D, 0.001 in.	$\Delta D$ 0.001 in.	Fibre Strain in./in.	Remarks
<u>Specimen 201-C</u>				
0	0	0		
100	9	0		
200	22	0		
300	40	3.5		
400	59	8.5		
500	80	11		
600	102	15		
700	121	19	0.0024	First visible crack.
840	148	21		
920	169	24.5		
1000	198	28		
1100	246	34		Rods slipping.
<u>Specimen 201-A</u>				
0	0	0		
100	15	0		
200	29	1		
300	46	2.5		
400	67	6		
500	87	9		
600	107	11.5	0.0022	First visible crack.
700	125	14		
800	150	18		
900	177	21		
1000	203	25		
1100	245	28		Rods slipping.
<u>Specimen 201-F</u>				
0	0	0		
100	11	0		
200	30	2.5		
300	49	4.5		
400	70	8		
500	93	11		
600	114	13		
700	140	17	0.0023	First visible crack.
800	168	21		
900	200	27		
1000	240	30		
1100	299	34		
1200	393	41		
1250	430	41		

TABLE 12. Continued.

Load lb	Midspan Deflection D, 0.001 in.	$\Delta D$ 0.001 in.	Fibre Strain in./in.	Remarks
<u>Specimen 201-B</u>				
0	0	0		
100	10	0		
200	24	1.5		
300	39	4		
400	53	5		
500	71	9	0.0013	First visible crack.
600	91	12		
700	112	15		
800	132	18		
900	155	21		
1000	180	25		
1100	211	29		
1200	280	55		
1250	330	42		
<u>Specimen 201-G</u>				
0	0	0		
100	15	0		
200	29	2.5		
300	41	3.5		
400	57	6		
500	78	8.5	0.0013	First visible crack.
550	128	13		
780	411	50		
<u>Specimen 201-H</u>				
0	0	0		
100	10	0		
200	23	0.5		
300	42	4		
400	61	7		
500	86	14		
600	105	18	0.0018	First visible crack 540 lb.
700	131	26		
800	275	42		Rods slipping.
860	303	67		

TABLE 12. Continued.

Load lb	Midspan Deflection D, 0.001 in.	$\Delta D$ 0.001 in.	Fibre Strain in./in.	Remarks
<u>Specimen 202-2</u>				
0	0	0		
100	14	0		
200	35	5		
300	53	6		
400	75	11		
500	94	15	0.0015	First visible crack.
600	114	19		
700	138	22		
800	165	27		
900	193	29		
1000	222	37		
1100	259	43		
1200	292	46		
1300	348	55		
1400	411	66		
1440	-	-		
<u>Specimen 202-1</u>				
0	0	0		
100	19	2		
200	39	6.5		
300	60	8.5		
400	75	11		
500	98	16		
600	125	19		
700	148	22		
800	170	25	0.0024	First visible crack.
900	202	32		
1000	232	34		
1100	264	38		
1200	300	42		
1300	344	50		
1400	415	58		
1440	-	-		

TABLE 13. WIDTH OF CRACKS DEVELOPED IN BENDING IN  
SPECIMENS SUBSEQUENTLY IMMERSSED IN SEA-  
WATER FOR TWO MONTHS.

Crack Width, mm			
201-C	201-F	201-G	202-2
0.07	0.25	0.05	0.15
0.10	0.10	0.40	<0.05
0.03	0.30	0.65	0.40
0.01	0.35	0.55	0.20
			0.15
			0.25

TABLE 14. PAINT SYSTEMS EXPOSED TO MARINE ENVIRONMENT

Half-Panel No.	Etched in HCl	Description of Paint System Used	Total Coat Thickness mils
3A	Yes	Primer - Inorganic two-component self-curing ethyl silicate zinc-rich primer Dried 6 hr in normal laboratory environment. Top coat - same as primer coat.	6
6	Yes	Primer seal coat - Two-component clear epoxy finish. Dried 8 hr in normal laboratory environment. Top coats - vinyl resin base anti-fouling paint. Dried 4 hr. - vinyl resin base anti-fouling paint.	4
7	Yes	Primer seal coat - Chlorinated rubber-based paint thinned with 15 percent thinner. Dried 8 hr. Top coats - Chlorinated rubber-based paint. - Chlorinated rubber-based paint.	4
9A	Yes	Primer seal coat - Zinc silico-fluoride solution. Dried 16 hr. Top coat - Steelmate - a highly-modified polyester resin vehicle containing metal and metallic oxide fillers.	4
9B	Yes	Primer seal coat - None. Top coat - Steelmate (as in 9A).	4
11A	Yes	Primer seal coat - Polyvinyl chloride-based enamel coating thinned with 15-percent vinyl thinner. Dried 2 1/2 hr. Top coats - Polyvinyl chloride-based enamel. Dried 2 1/2 hr. - Polyvinyl chloride-based enamel coating.	5
11B	Yes	Primer seal coat - None. Top coats - Two-component pigmented epoxy-resin coating. Dried 5 1/2 hr. - Two-component pigmented epoxy-resin coating.	4

TABLE 14. Continued

Half-Panel No.	Etched in HCl	Description of Paint System Used	Total Coat Thickness mils
12A	Yes	Primer seal coat - Inorganic two-component self-curing ethyl silicate zinc-rich primer. Dried 6 hr. Top coat - Two-component clear chemical curing polyamide resin.	6
12B	Yes	Primer seal coat - Inorganic two-component self-curing ethyl silicate zinc-rich primer. Dried 6 hr. Top coat - Polyvinyl chloride-based enamel thinned with 30-percent vinyl thinner.	6
13	No	Primer seal coat)- As in panel No. 6. However top coats broke badly and specimens Top coats ) were not exposed to environment tests.	
14	No	Primer seal coat)- As in panel No. 7. Top coats )	4
16A	Yes	Primer seal coat - Clear chemical during polyamide resin. Dried 24 hr. Top coat - Two-component clear chemical curing polyamide resin.	5
16B	Yes	Primer seal coat - Chlorinated rubber-based enamel thinned with 15-percent compatible thinner. Dried 24 hr. Top coats - Chlorinated rubber-based enamel. Dried 24 hr. - Chlorinated rubber-based enamel.	4

TABLE 15. CONDITIONS OF SPECIMENS AFTER SECOND PERIOD OF MARINE TIDAL EXPOSURE - 150 DAYS AT LOW-LOW TIDE

Specimen No.	Paint System Used	Condition
3	Prime and top coat - inorganic two-component self-curing ethyl silicate zinc rich-paint.	No barnacles.
6	Primer - two-component clear epoxy finish. Top coat - two coats of vinyl resin base anti-fouling paint.	No barnacles.
7	Primer - thinned chlorinated rubber-based paint. Top coat - two coats of chlorinated rubber-based paint.	Bases of barnacles did not damage paint but are difficult to scrape off without paint damage.
9A	Primer - sealed with zinc silico-fluoride solution. Top coat - a highly-modified polyester resin/metal/oxide.	Barnacles completely dissolved paint around base and partly under base.
9B	Primer - no seal coat Top coat - as in 9A	As in 9A.
11A	Primer - thinned polyvinyl chloride-based enamel. Top coat - two coats polyvinyl chloride-based enamel.	As in 7.
11B	Primer - none. Top coat - two coats of two-component pigmented epoxy resin.	As in 7.
12A	Primer - inorganic two-component self-curing ethyl silicate zinc-rich primer. Top coat - two-component clear chemical curing polyamide resin.	Bases did not damage paint and could be scraped off with little damage to paint.
12B	Primer - as in 12A Top coat - thinned polyvinyl chloride-based enamel.	As in 7.
14	Primer - thinned chlorinated rubber-based paint. Top coat - two coats of chlorinated rubber-based paint.	As in 7.
16A	Primer - clear chemical curing polyamide resin. Top coat - two-component clear chemical curing polyamide resin.	As in 12A.
16B	Primer - thinned chlorinated rubber-based enamel. Top coat - two coats of chlorinated rubber-based enamel.	As in 7.

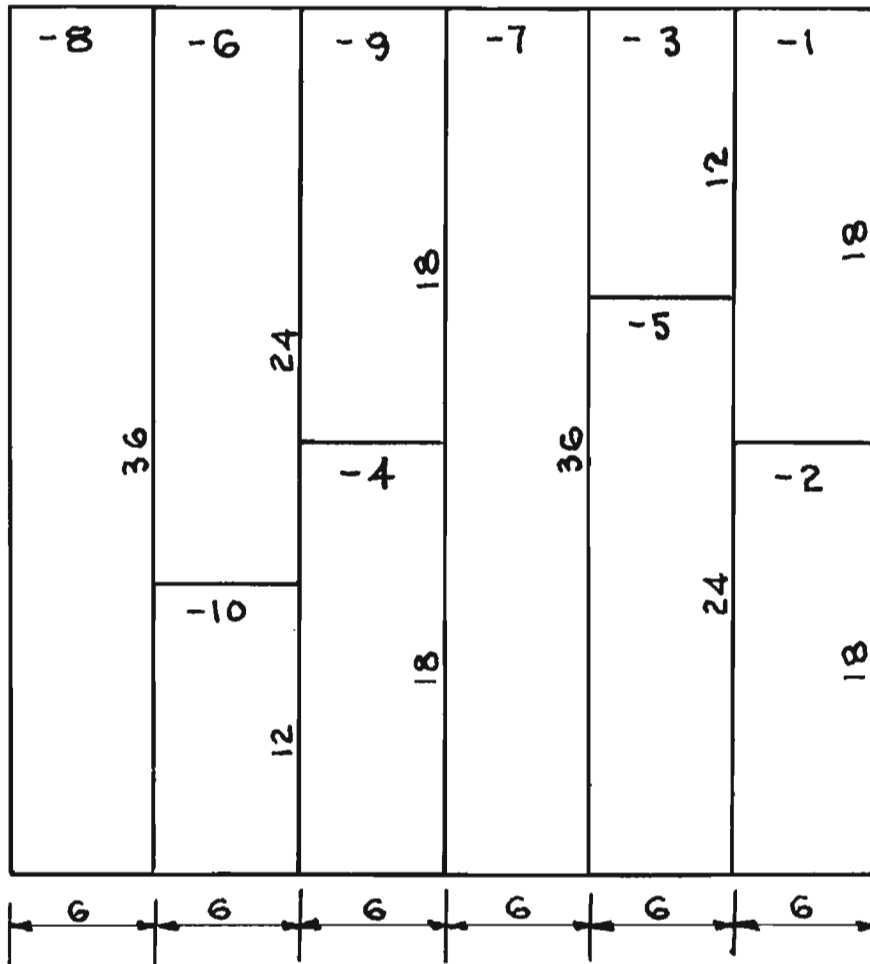


Fig. 1. Panel Layout for Flexure and Tensile Test Specimens.



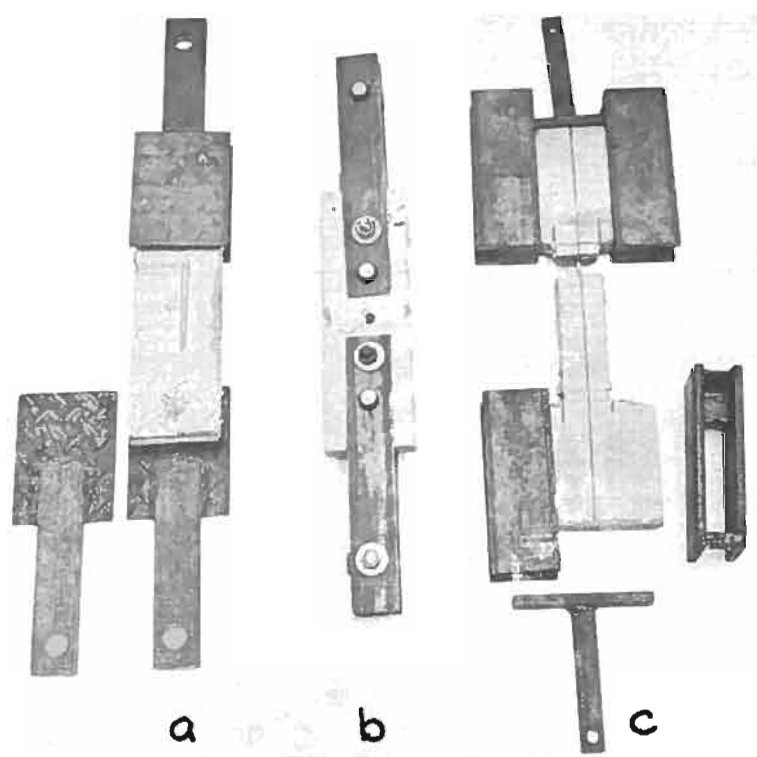
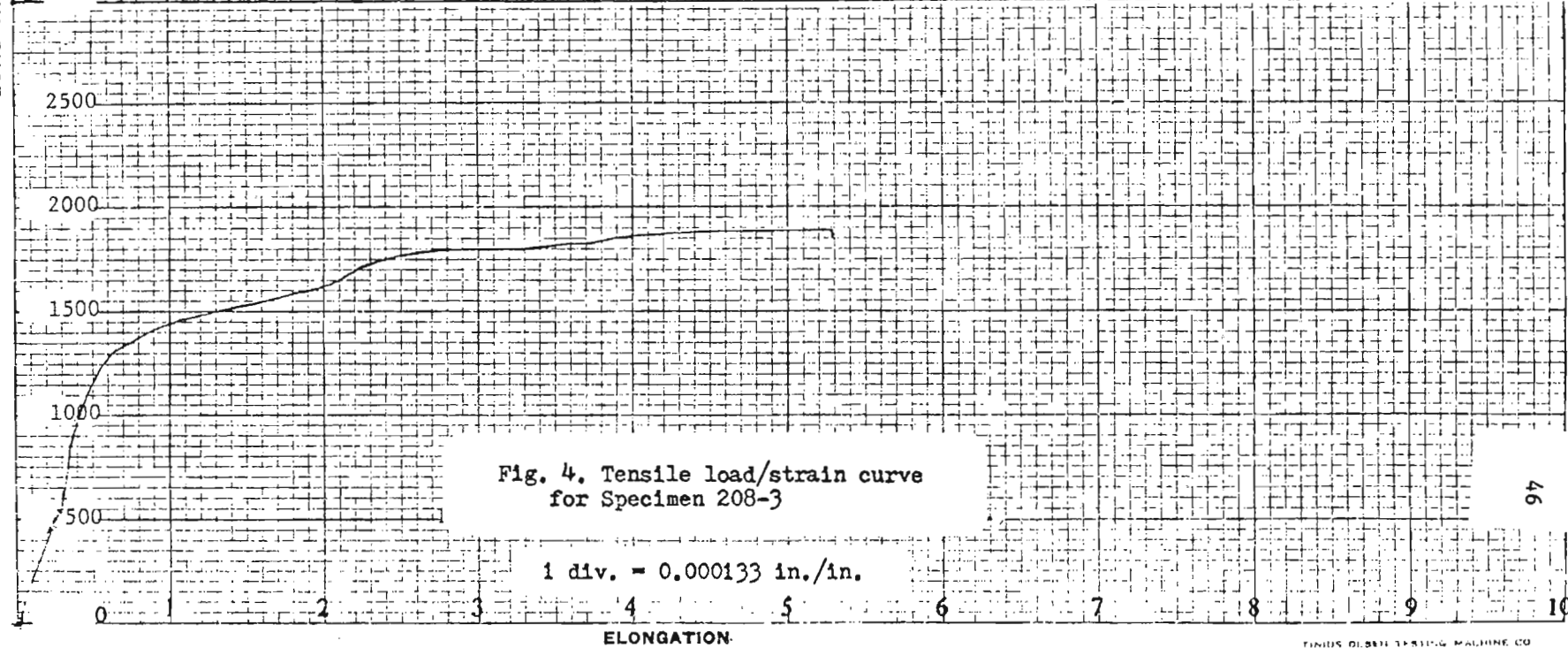
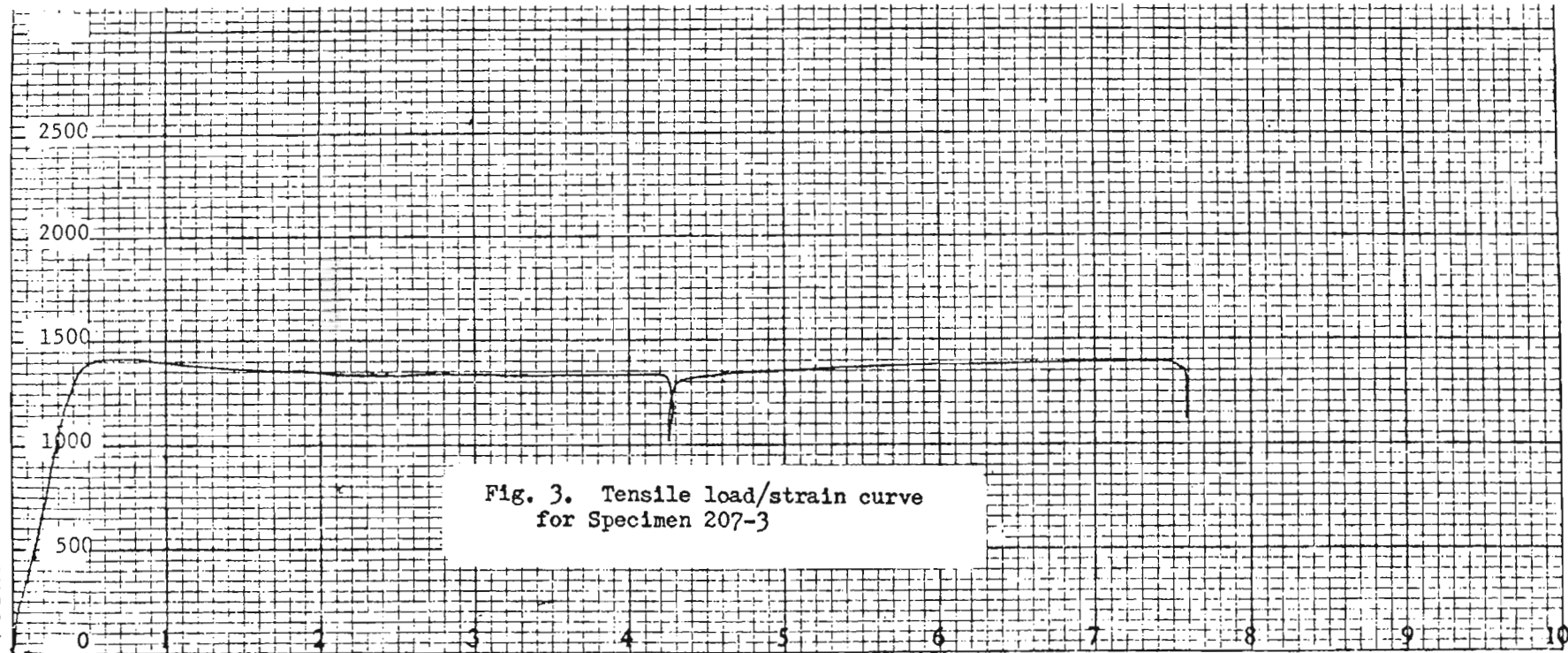


Fig. 2. Views of Tensile Specimens and Loading Grips Used.

Test No. } In  
 Elongation }  
 Compression }  
 Size } In  
 Area }  
 Yield Point lbs. Sq. In. }  
 Ultimate Str. lbs. Sq. In. }  
 Per Cent. Elongation }  
 Per Cent. Reduced Area }  
 Date }



Test No. } In  
 Elongation }  
 Compression }  
 Size. } Inches  
 Area }  
 Yield Point Lbs. Sq. In. }  
 Ultimate Str. Lbs. Sq. In. }  
 Per Cent. Elongation }  
 Per Cent. Reduced Area }  
 Date

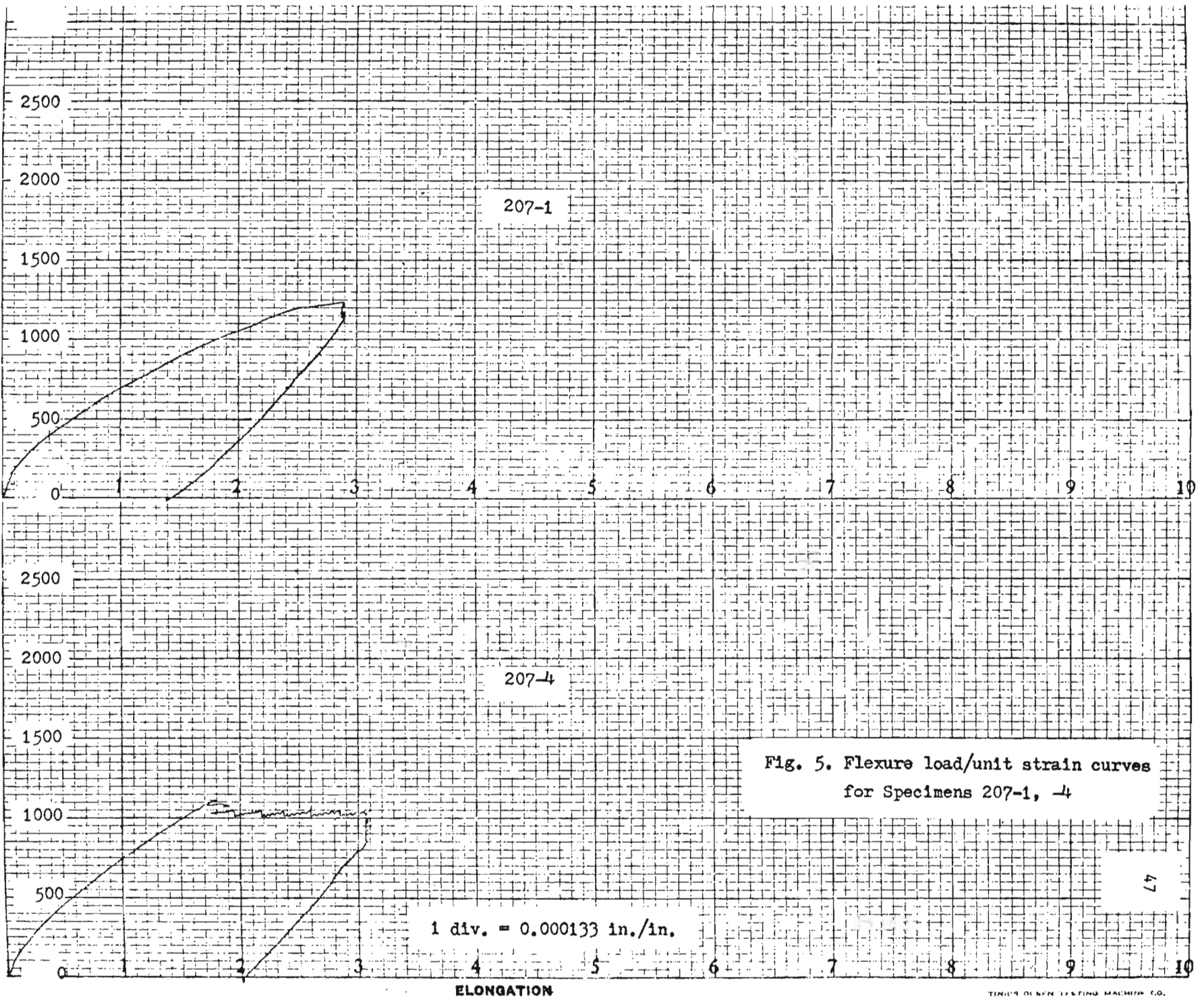


Fig. 5. Flexure load/unit strain curves for Specimens 207-1, 4

Test No. \_\_\_\_\_  
 Elongation }  
 Compression }  
 Size \_\_\_\_\_ In  
 Area \_\_\_\_\_  
 Yield Point Lbs. Sq. In. \_\_\_\_\_  
 Ultimate Str. Lbs. Sq. In. \_\_\_\_\_  
 Per Cent. Elongation \_\_\_\_\_  
 Per Cent. Reduced Area \_\_\_\_\_  
 Date \_\_\_\_\_

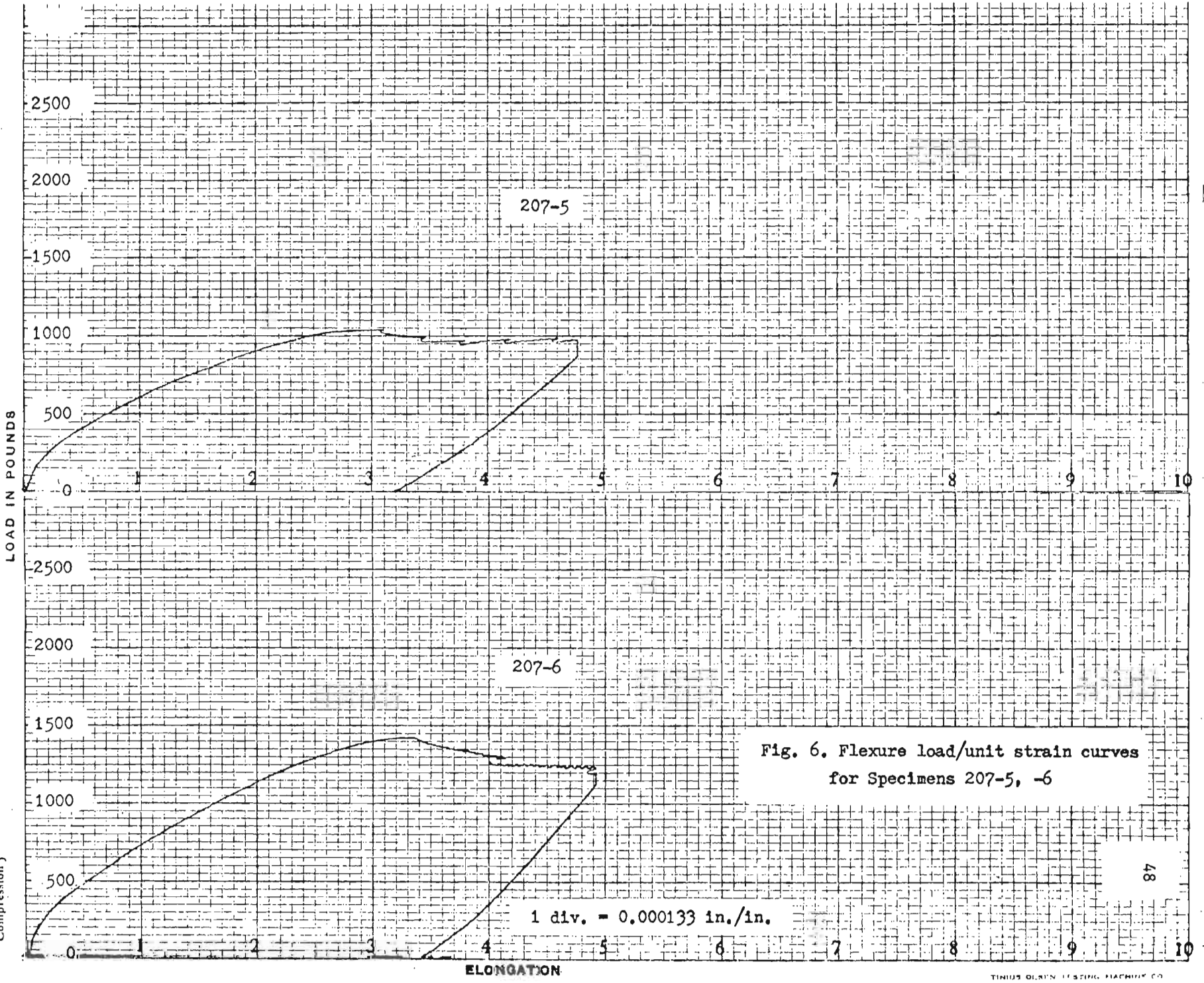


Fig. 6. Flexure load/unit strain curves for Specimens 207-5, -6

Test No. { Elongation } in  
 Compression }  
 Size } in  
 Area }  
 Yield Point Lbs. Sq. In. Per Cent. Elongation  
 Ultimate Str. Lbs. Sq. In. Per Cent. Reduced Area Date

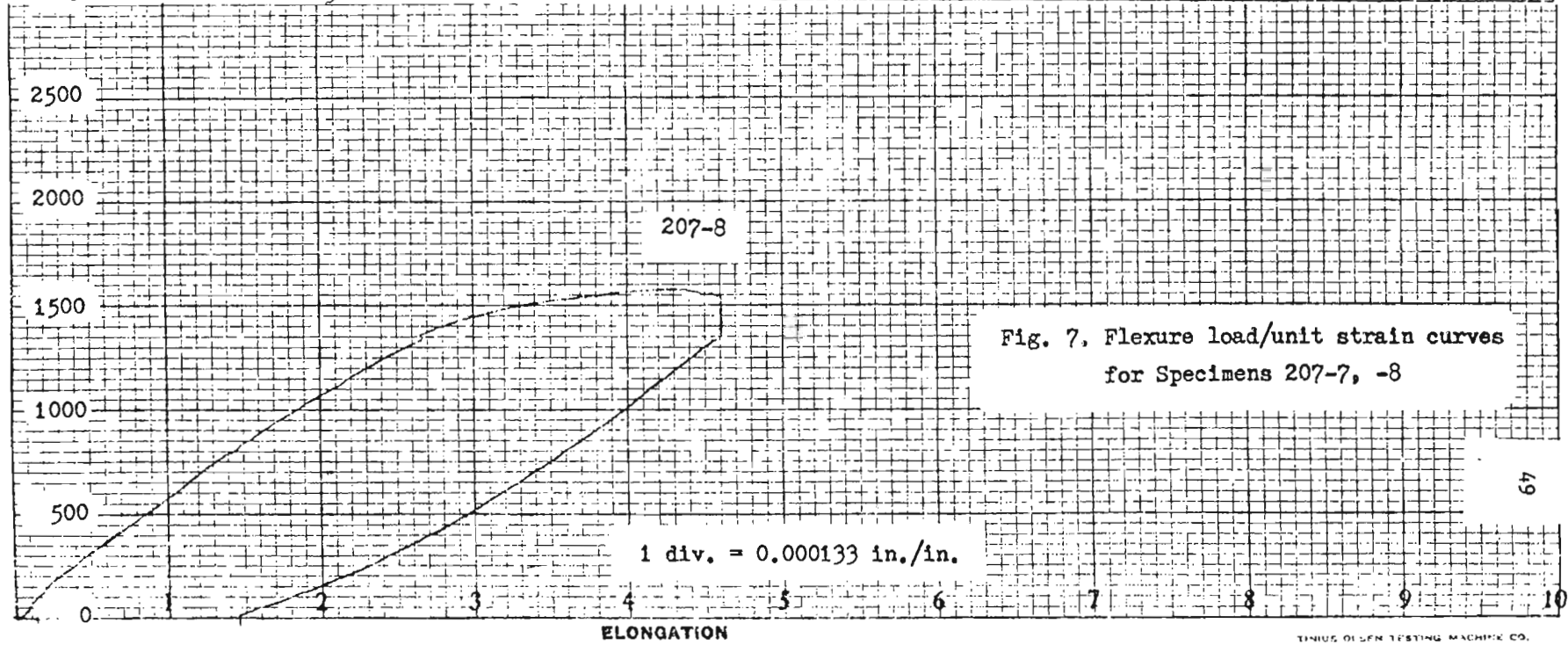
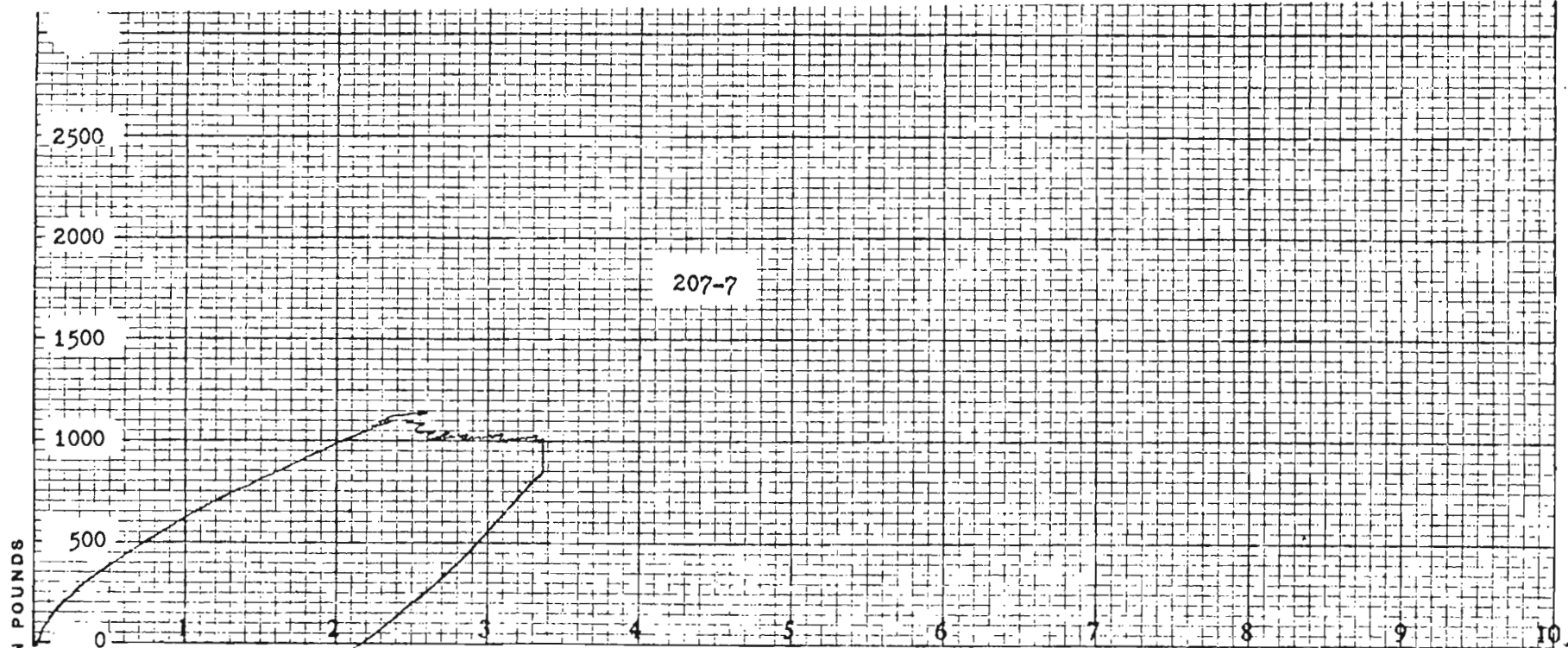


Fig. 7. Flexure load/unit strain curves for Specimens 207-7, -8

Test No. \_\_\_\_\_ Size \_\_\_\_\_ Area \_\_\_\_\_ Yield Point Lbs. Sq. In. \_\_\_\_\_ Ultimate Str. Lbs. Sq. In. \_\_\_\_\_  
 Elongation } In \_\_\_\_\_ Inches \_\_\_\_\_ Per Cent. Elongation \_\_\_\_\_ Per Cent. Reduced Area \_\_\_\_\_ Date \_\_\_\_\_  
 Compression }

LOAD IN POUNDS

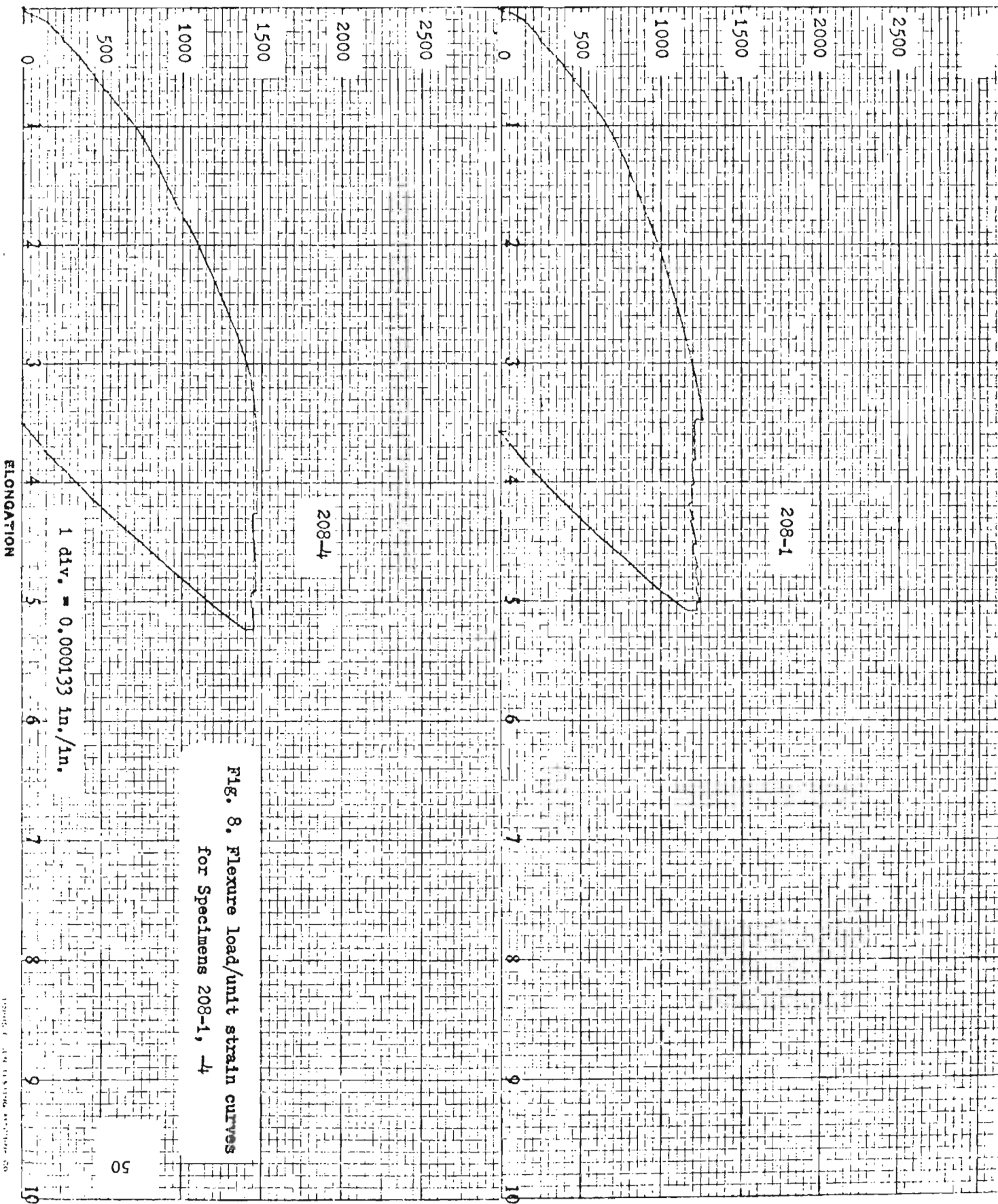


Fig. 8. Flexure load/unit strain curves for Specimens 208-1, 4

Text No. } In  
 Elongation }  
 Compression }  
 Size } In  
 Area }  
 Yield Point Lbs. Sq. In. }  
 Ultimate Str. Lbs. Sq. In. }  
 Date }  
 Per Cent. Elongation }  
 Per Cent. Reduced Area }

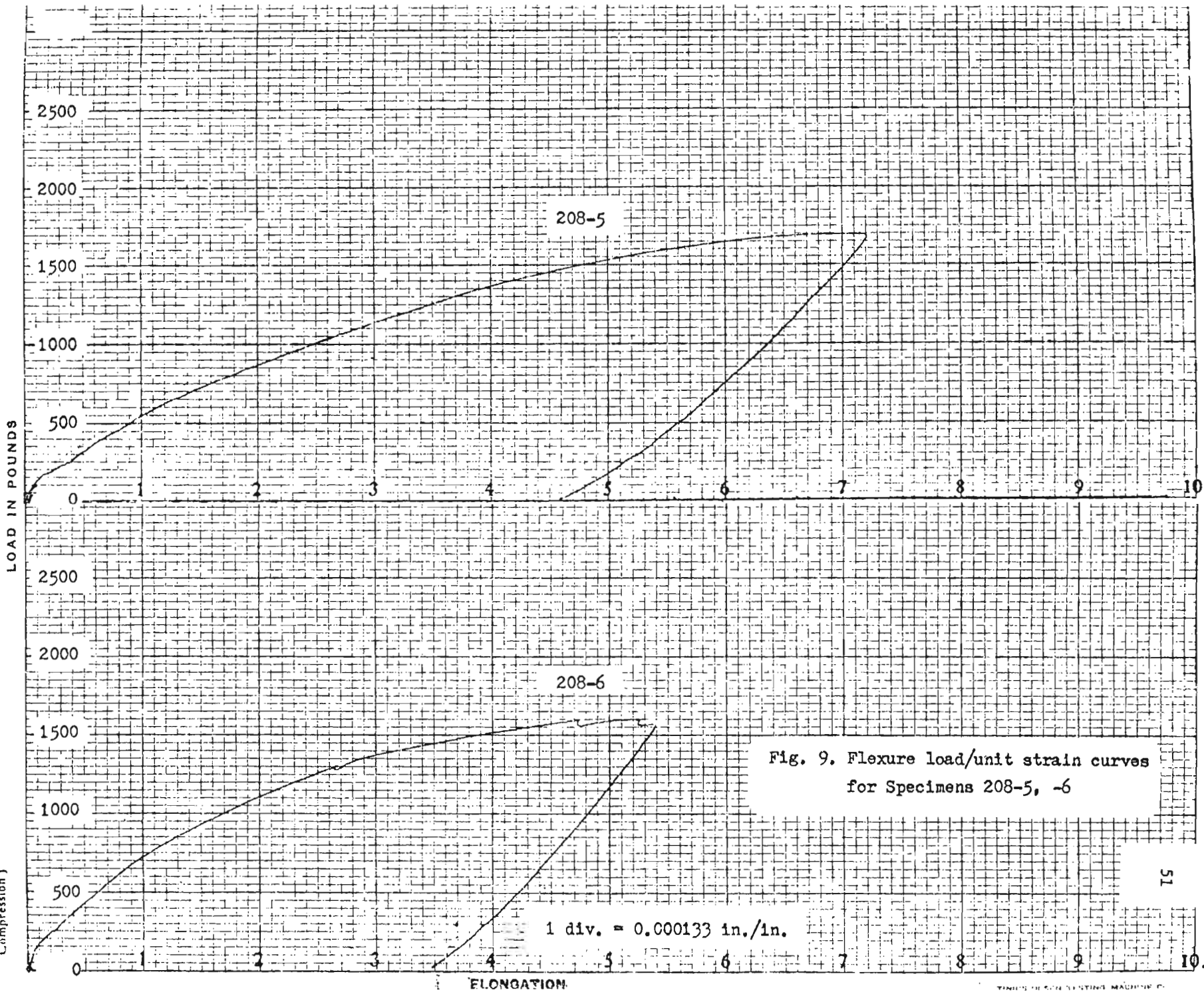


Fig. 9. Flexure load/unit strain curves for Specimens 208-5, -6

Test No. { Elongation / Compression } In  
 Size Inches  
 Area  
 Yield Point Lbs. Sq. In. Per Cent. Elongation  
 Ultimate Str. Lbs. Sq. In. Per Cent. Reduced Area  
 Date

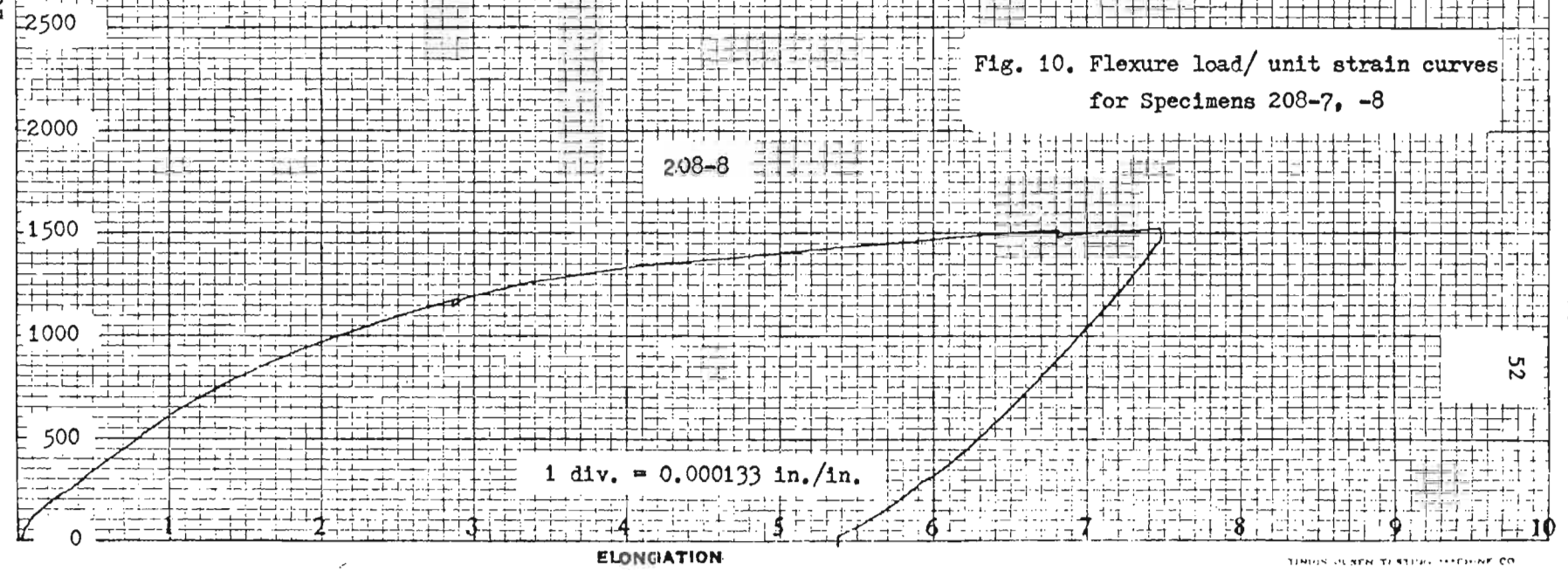
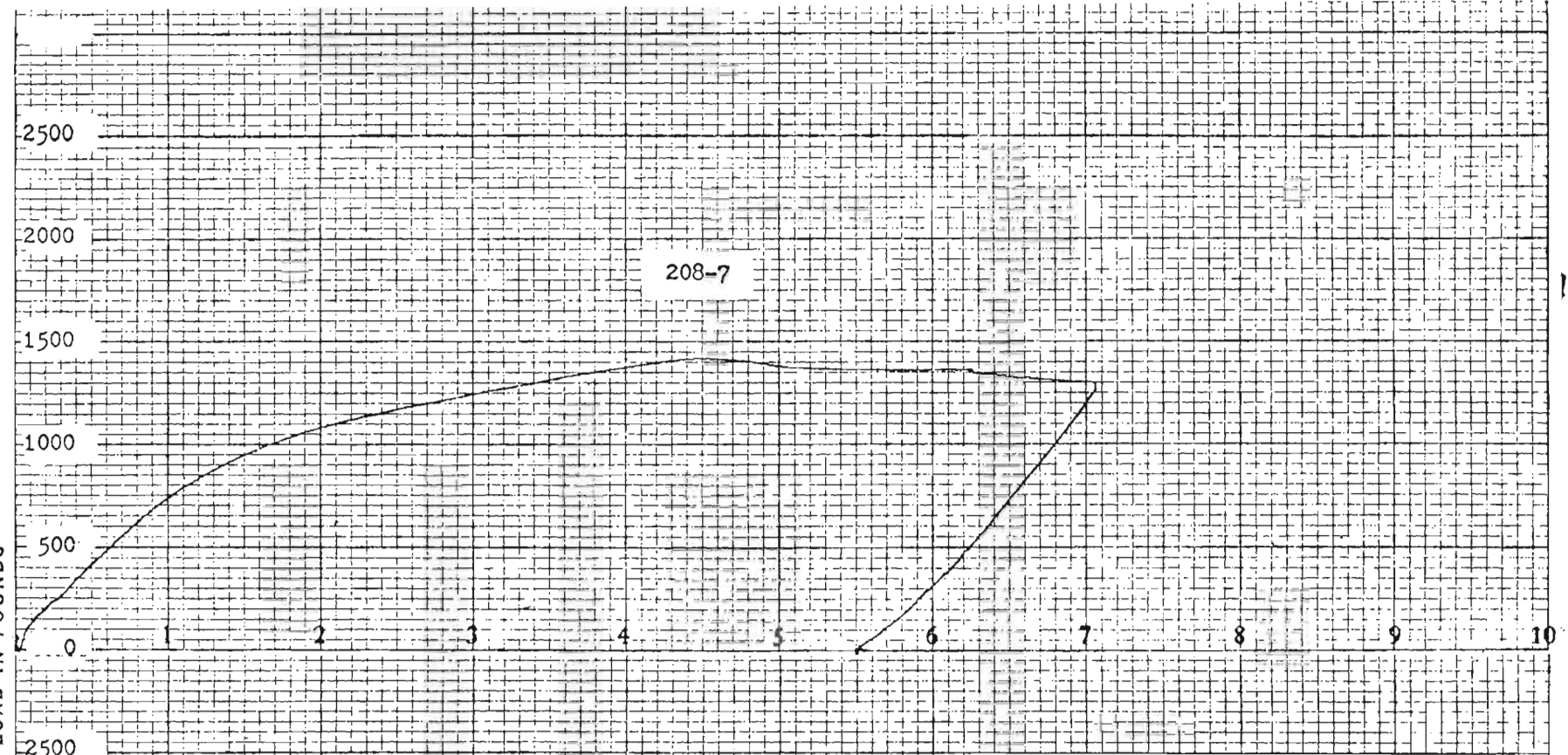


Fig. 10. Flexure load/ unit strain curves for Specimens 208-7, -8



LOAD IN POUNDS

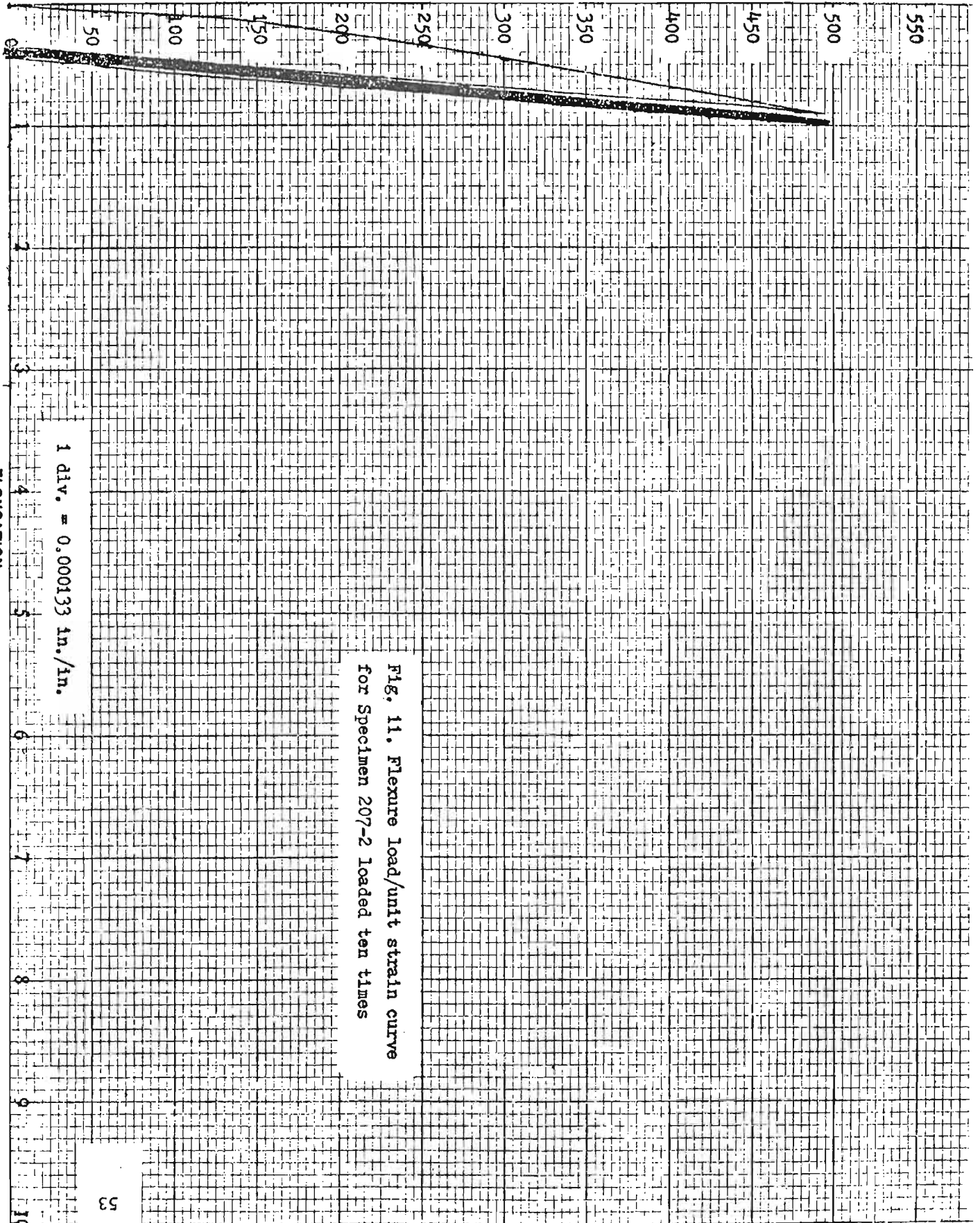


Fig. 11. Flexure load/unit strain curve  
for Specimen 207-2 loaded ten times

1 div. = 0.000133 in./in.

ELONGATION-

Text No. \_\_\_\_\_  
 Elongation } In \_\_\_\_\_  
 Compression }  
 Size \_\_\_\_\_  
 Area \_\_\_\_\_  
 Yield Point Lbs. Sq. In. \_\_\_\_\_  
 Per Cent. Elongation \_\_\_\_\_  
 Ultimate Str. Lbs. Sq. In. \_\_\_\_\_  
 Per Cent. Reduced Area \_\_\_\_\_  
 Date \_\_\_\_\_

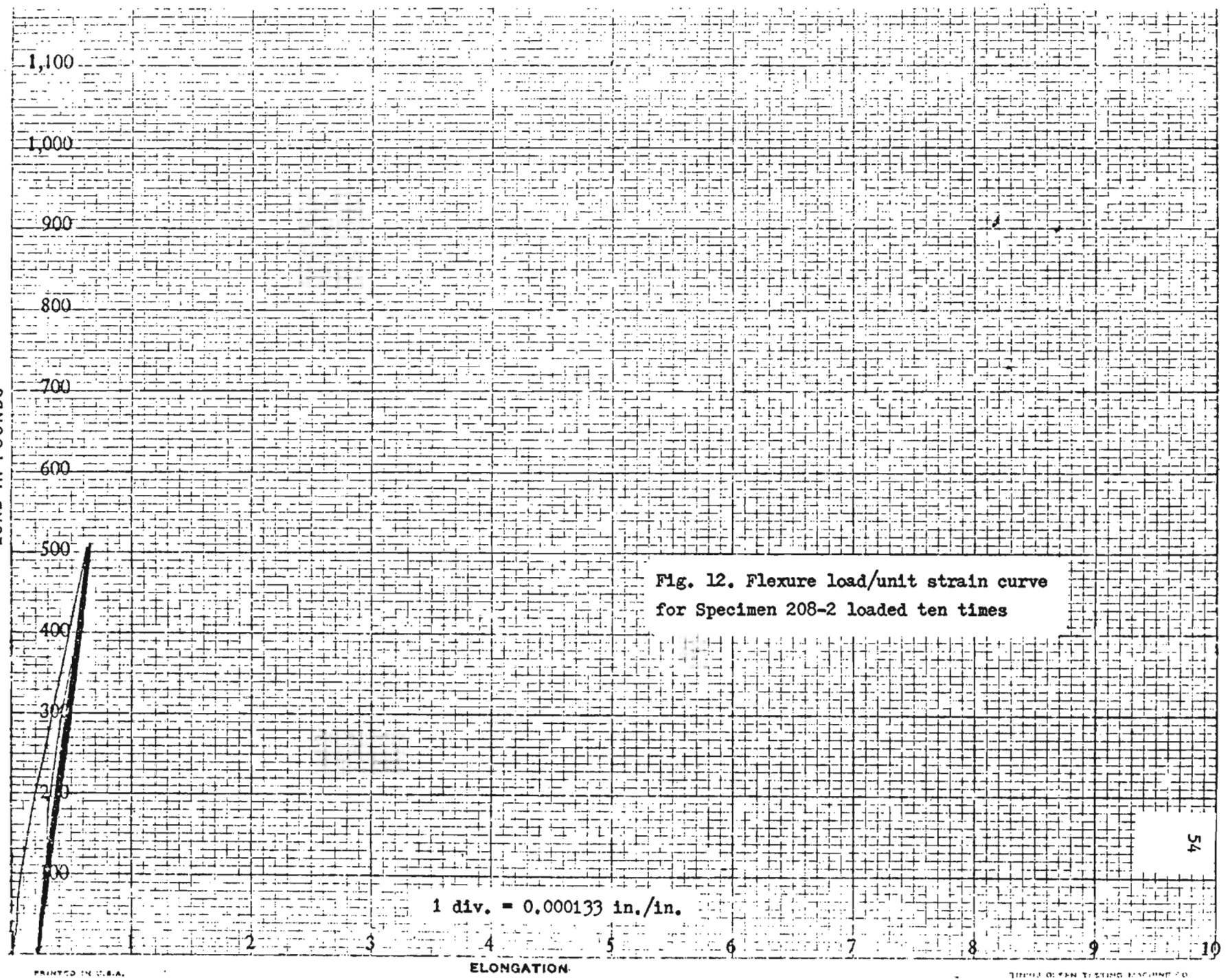
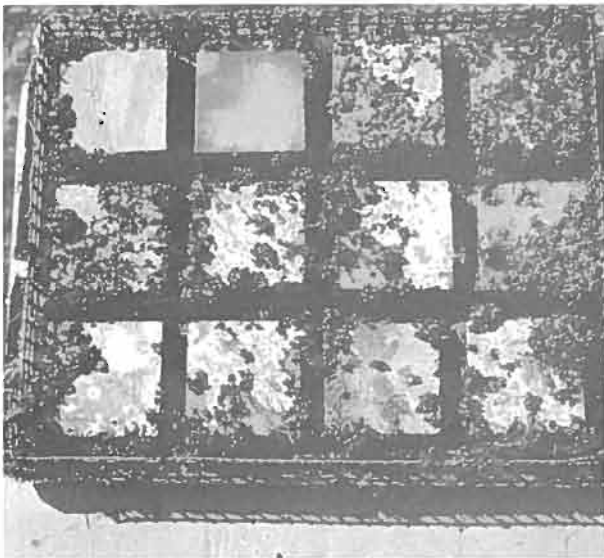
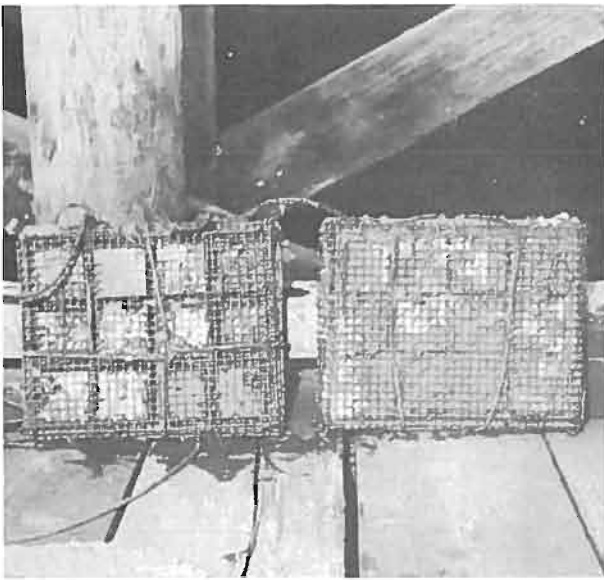


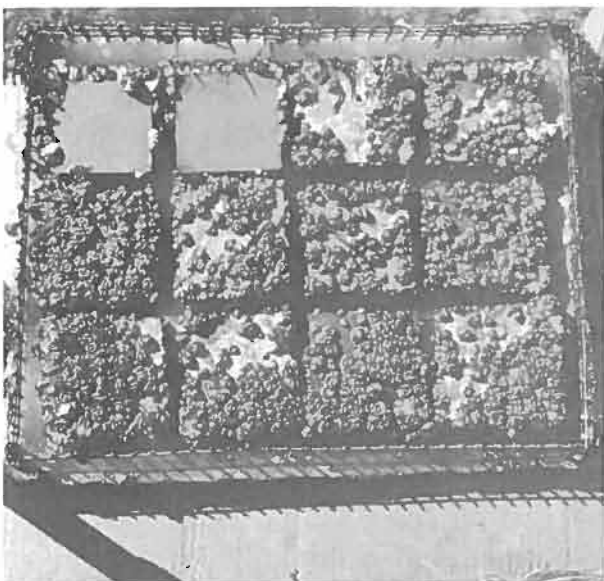
Fig. 12. Flexure load/unit strain curve for Specimen 208-2 loaded ten times

Fig. 13, 14, 15. Painted Specimens  
exposed 230 Days at  
Vancouver-Kitsilano.

Left - at mean tide.  
Right - at low-low tide.



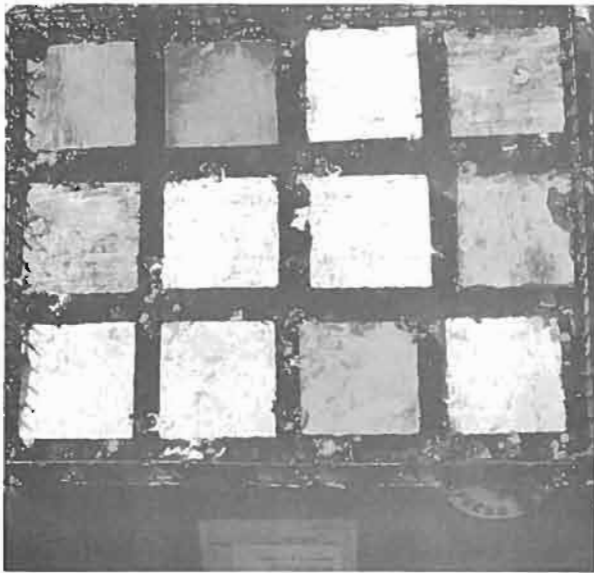
At mean tide.



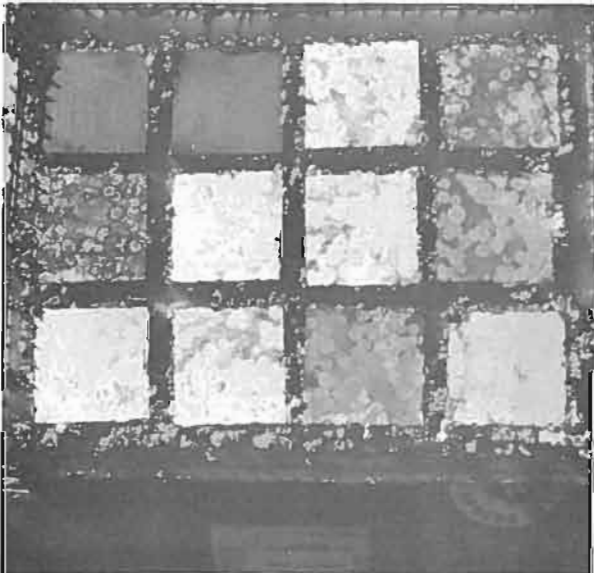
At low-low tide.

Fig. 16, 17.

Painted Specimens  
exposed 230 Days at  
Vancouver-Kitsilano.



At mean tide.



At low-low tide.

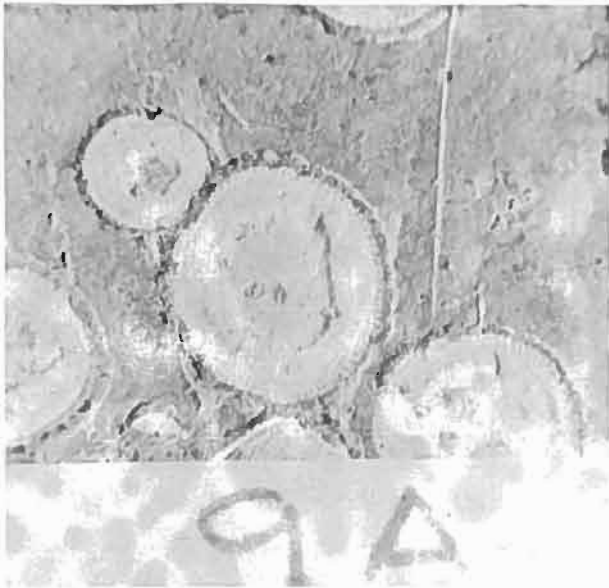


Fig. 18. View showing Paint removed from Area around and under Barnacle Pad.

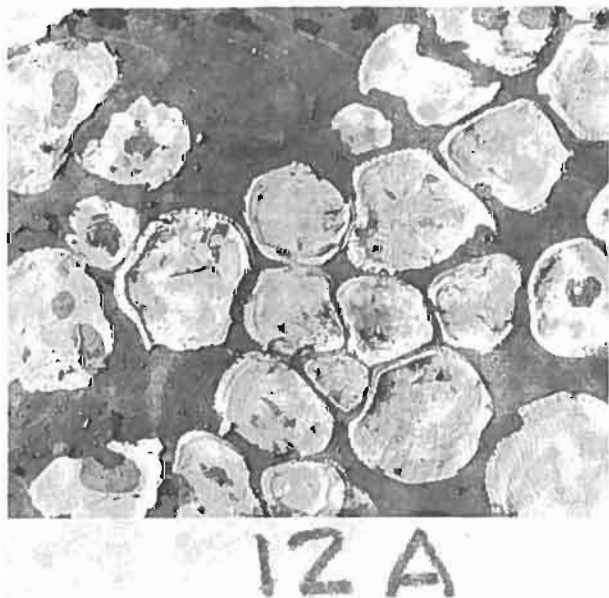


Fig. 19. View showing Paint not removed from Area around and under Barnacle Pad.